VECTOR WIND PROFILE GUST MODEL

FINAL REPORT

(For Period April 10, 1979 – April 9, 1980)

Prepared For

NATIONAL AERONAUTICS AND SPACE ADMINISTRATION
George C. Marshall Space Flight Center
Marshall Space Flight Center, Alabama 35812

Under Contract NAS8-33433

(NASA-CR-161475) VECTOR WIND PROFILE GUST MODEL Final Report, 10 Apr. 1979 - 9 Apr. 1980 (Computer Sciences Corp.) 65 p
HC A04/MF A01 CSCL 04B

N80-25993

Unclas
G3/47 23466

CSC

COMPUTER SCIENCES CORPORATION

VECTOR WIND PROFILE GUST MODEL

FINAL REPORT

(For Period April 10, 1979 – April 9, 1980)

Contract NAS8-33433

April 9, 1980

Prepared By

Stanley I. Adelfang
Beverly A. Evans
Computer Sciences Corporation
300 Sparkman Drive, NW, Wing E
Huntsville, Alabama 35805
205/837-5750

Prepared For

National Aeronautics and Space Administration
George C. Marshall Space Flight Center
Marshall Space Flight Center, Alabama 35812

TABLE OF CONTENTS

LIST OF ILLUSTRATIONS

LIST OF ILLUSTRATIONS (CONT'D.)

LIST OF ILLUSTRATIONS (CONT'D.)

LIST OF ILLUSTRATIONS (CONT'D.)

LIST OF TABLES

SECTION I. INTRODUCTION

This report summarizes the work during a 12-month study to establish and apply analytical techniques for development of a vector wind profile gust model for the Space Transportation System OFT Operations and Trade Studies.

Jones (Ref. 1) summarizes the fundamental issue involved in application of gust models for evaluation of vehicle structural response. Basically, vehicle structures can be considered to be either highly damped or slightly damped. Highly damped modes are associated with vehicle control and handling qualities; large response of these modes can be generated by imposing a single discrete gust with an appropriate length scale. On the other hand, large responses for slightly damped modes could be the cumulative effect of a sequence or cluster of gusts with an appropriate spacing or phasing; such a sequence of gusts is best treated with a power spectrum model.

The application of either model depends on which type of response mode is dominant. The inaccuracy of using one model and neglecting the other should be evaluated and taken into account. For example, when power spectra are used, analysis of the effect of the non-Gaussian structure of turbulence is necessary; when a discrete gust model is used, simple clustering of discrete gusts should be studied for possible resonance effects.

Jones concludes that analysis of large disturbances recorded during passage through patches of turbulence are usually associated with a single gust that stands out above the general level of roughness. It is implied that these large loads can be simulated with a discrete gust model.

From the above discussion, it is clear that a discrete gust model can be useful in studying the response of damped vehicle structures to turbulence. The results of this study will be suitable for modeling of discrete gusts in vertical wind profiles.

The body of this report is composed of three sections (II through IV). Section II describes basic and derived properties of the data analyzed in this study. Section III describes the calculation of wind gust data from Jimsphere wind profiles and the establishment of probability distributions of gusts in four wavelength bands. Conclusions are presented in Section IV.

SECTION II. DATA

This section describes basic and derived properties of the data analyzed in this study. Basic properties include the number, type, and location of the wind profiles; derived properties include an evaluation of the response of the measurement system at small wavelengths.

A. Data Sample

The data consist of 1800 Jimsphere profiles (150 per month) from Cape Kennedy, Florida (Ref. 2). The data were obtained from a Space Shuttle Level II directive that specifies the demonstration of vehicle design validity using 150 Jimsphere wind profiles representative of each month. Three months (February, April, and July) were chosen for analysis in this study. The February and July data are representative of the seasonal extremes at Cape Kennedy; the April data are representative of the transition between the extremes. The number of soundings for each month for each year of the sampling period is illustrated in Figure 1.

B. Wind Measuring System Amplitude Response

Wind profile data used in this study were obtained with the Jimsphere system. Since the small wavelength perturbations observed in these profiles are the subject of a detailed analysis, it is appropriate to specify the accuracy of the system for small wavelengths. A measure of the accuracy is the amplitude response, $G(\lambda)$, which is equivalent to the ratio $A(\lambda)/A^*(\lambda)$; where $A^*(\lambda)$ is the true amplitude of a perturbation in the wind profile at wavelength, λ, and $A(\lambda)$ is the amplitude measured with the Jimsphere system. The amplitude response of the Jimsphere system is limited by the size of the balloon (2-meter diameter), the balloon ascent rate (4-5 m/sec), the accuracy of the balloon tracking system (FPS-16), and the data smoothing technique. The balloon positions, determined every 0.1 second, are smoothed to provide mean positions at each 25-meter interval of ascent. Differences in position between alternate 25-meter levels indicate the mean wind for the corresponding 50-meter layer, and are reported as the wind at the 25-meter level in the middle of the 50-meter layer. Thus, the basic data analyzed here are wind speeds and directions for 50-meter layers, overlapping

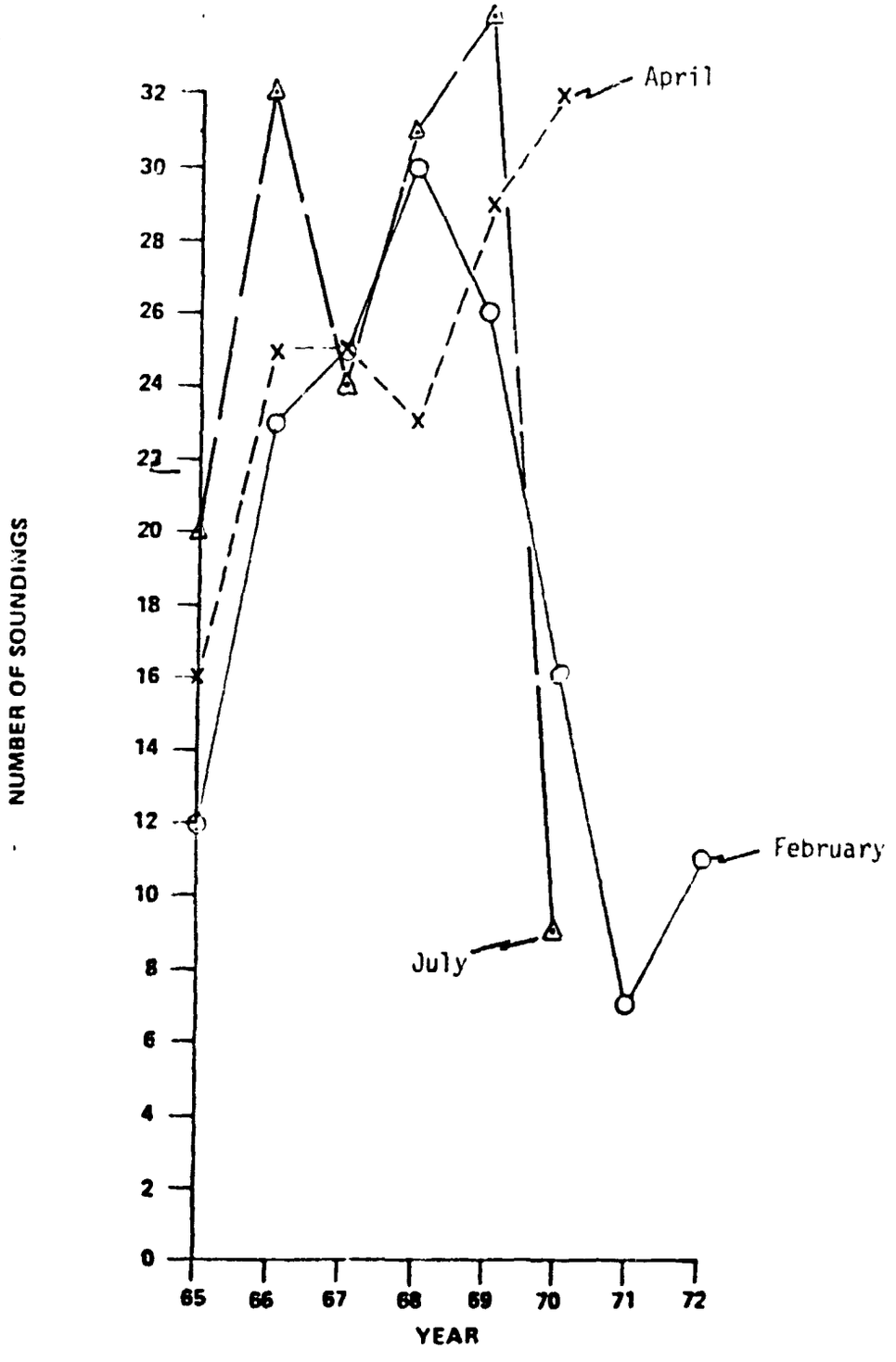

Figure 1. Distribution of February, April, and July Jimsphere Soundings from 150 per Month Sample (Ref. 2.

by 25 meters. Only when at least 25 meters intervene between two layers (i.e., winds reported for levels at least 75 meters apart) can two winds be considered independent observations (Ref. 3).

Expressions for the amplitude response, $G(\lambda)$, of the Jimsphere system to wind perturbation wavelengths that are small relative to the length of the wind profile have been derived by Luers and Engler (Ref. 4),

$$G(\lambda) = \frac{\cos\left(\frac{\pi S}{3\lambda}\right) \sin^2\left(\frac{\pi S}{3\lambda}\right)}{\left(\frac{\pi S}{3\lambda}\right)^2} \qquad (1)$$

and by DeMandel and Krivo (Ref. 5),

$$G(\lambda) = \frac{\sin\left(\frac{4\pi w}{\lambda}\right) \sin\left(\frac{50\pi}{\lambda}\right)}{200w\left(\frac{\pi}{\lambda}\right)^2} \qquad (2)$$

where

S = smoothing interval = 75m

λ = wavelength (m)

w = Jimsphere balloon ascent rate (m/s)

As illustrated in Fig. 2, the Jimsphere system does not measure wavelengths less than 50 meters; for λ=90m, the measured amplitude is one-half the true amplitude.

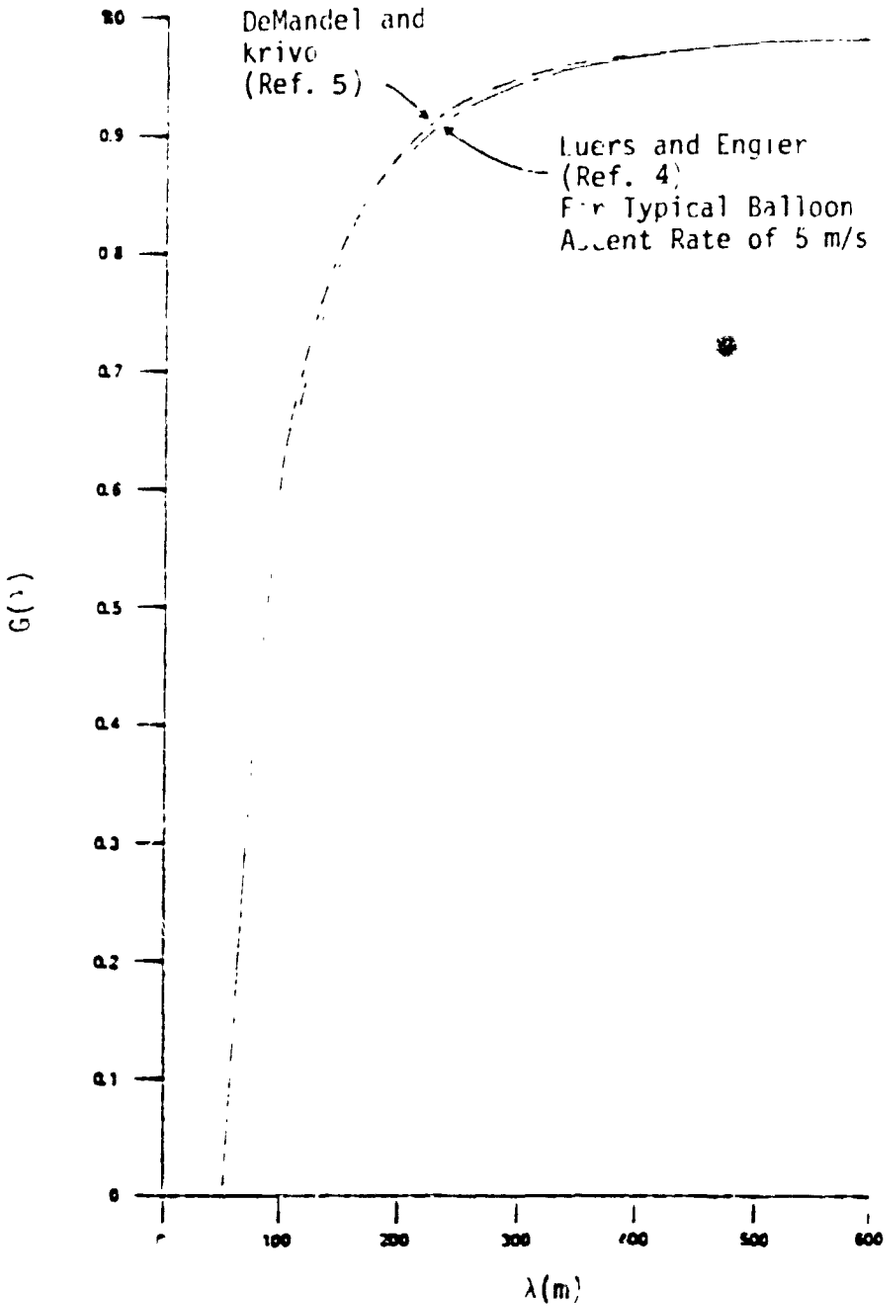

Figure 2. Amplitude Response of the Jimsphere System

SECTION III. WIND ANALYSIS

This section describes the calculation of wind gust data from Jimsphere wind profiles and the establishment of probability distributions of gusts. Sample estimates of the required parameters of the theoretical distribution functions are calculated and the variability of the parameters as a function of altitude, season, and gust wavelength range is established. Empirical functions for estimation of gust statistics for other wavelength ranges are derived.

A. DIGITAL FILTERS

Vector wind gust statistics and models are based on data that have been obtained from filtered wind profiles. The filtering process provides profile data that contain perturbations within a range of wavelengths that is suitable for simulation studies of space vehicle ascent through the atmosphere. The design and application of these filters are described below.

1. Filter Design. The design of the digital filters is based on the Martin-Graham cosine rolloff model described by Demandel and Krivo (Ref. 6). A set of numerical smoothing weights is calculated for a low-pass filter from the equation

$$h(nT) = \frac{\sin(2\pi f_t nT) + \sin(2\pi f_c nT)}{2\pi nT\left[1 - 4n^2T^2(f_t - f_c)^2\right]} \qquad (3)$$

where the filter design parameters are

T = altitude interval of wind profile data

n = weight index (-N, -N+1, ..., -1, 0, 1, ..., N-1, N)

N = (NW-1)/2

NW = number of weights

f_c = cutoff frequency = the highest frequency with associated amplitude passed with unity gain

f_t = termination frequency = the lowest frequency with associated amplitude passed with zero gain.

The center weight (n = 0) is given by:

$$h_0 = f_c + f_t. \tag{4}$$

When the weights, h_n, have been determined, they are normalized by applying the constraint

$$\sum_{N=-1}^{N} h_n = 1. \tag{5}$$

Only (N + 1) weights are calculated since $h_n = h_{-n}$. Since the filter function is symmetrical, no phase shift is produced.

The use of digital smoothing weights results in the loss of the first and last N data points of the original profile. Thus the filtered wind profile has an altitude range that is reduced by 2NT compared to the original profile.

The effective response of the low-pass filter, given the design parameters listed under equation (3) is

$$G_L(f) = h_0 + 2 \sum_{n=1}^{N} h_n \cos(2\pi f n T). \tag{6}$$

As the number of weights (NW) is increased, the response of the filter improves. However, computation time increases as does the number of points lost (the first and last N data points). In this study, NW was chosen to minimize data loss while maintaining a reasonably accurate filter response.

2. Filter Application. Jimsphere wind profiles from the surface to 20 km in component form (zonal and meridional) were decomposed into eight data bases by the filtering process diagrammed in Figure 3. Four of the data bases consist of low-pass profiles that can be used in analyses of steady state and wind bias profiles. The other data bases consist of high-pass profiles defined here as residual profiles; these profiles consist of perturbations with relatively small wavelengths that are of interest in evaluations of vehicle response. Gusts that are derived from residual profiles are the subject of the detailed statistical analysis described in subsequent sections of this report.

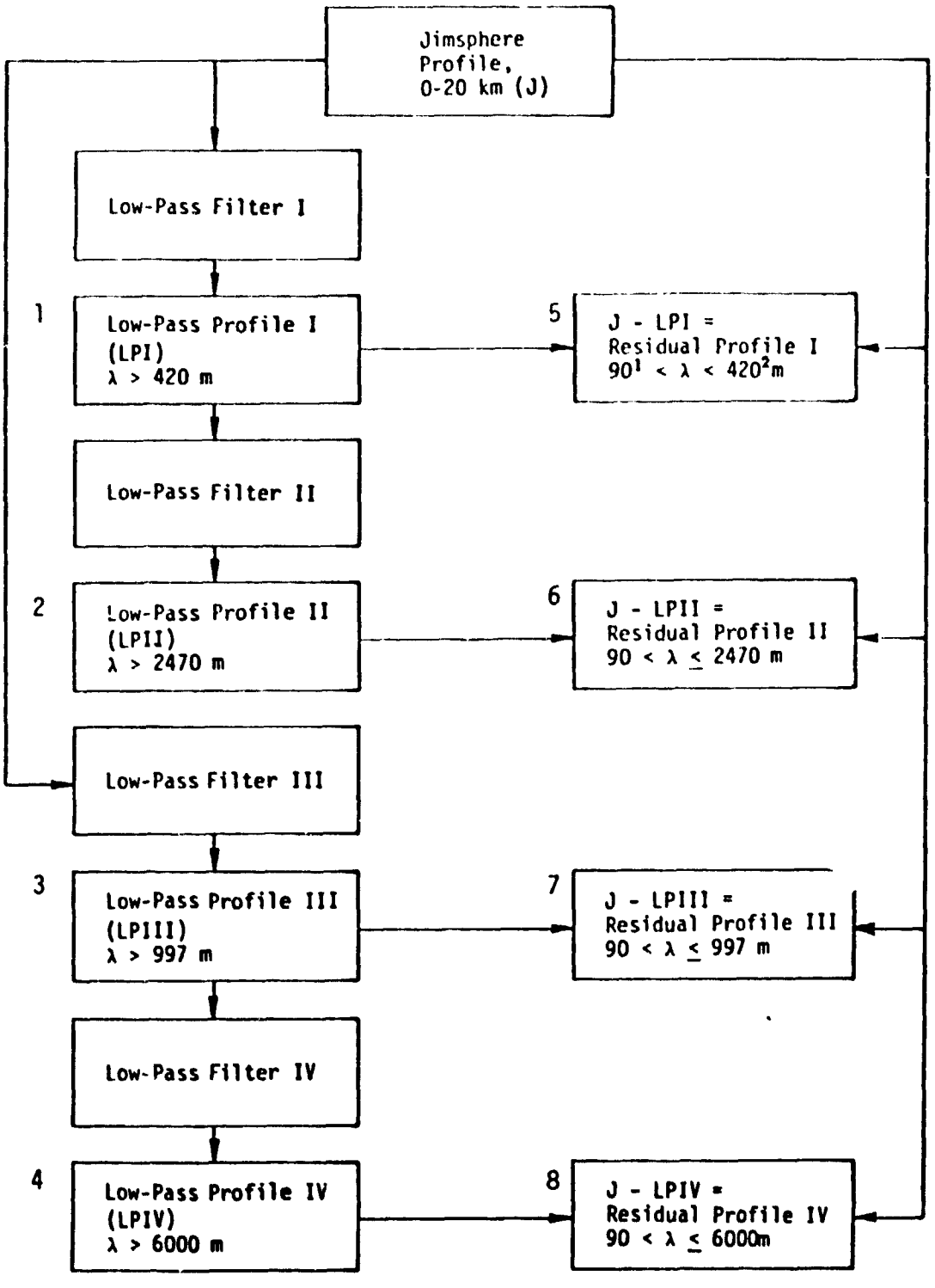

[1]Nominal low wavelength limit of Jimsphere system

[2]Defined in text

Figure 3. Filtering Process

The design parameters and weighting functions of four low-pass filters and the altitude range of the filtered profiles used in this study are listed in Table 1.

The method of calculating high-pass profiles by subtraction of the low-pass filtered profiles from the original Jimsphere profile is equivalent to the execution of a high-pass filter. The effective amplitude response of the four high-pass filters that are appropriate for description of the upper end of the wavelength range of the residual profiles is illustrated in Figure 4. The nominal high wavelength limit for each set of residual profiles is the wavelength at which the amplitude response of the corresponding filter is .50.

A set of u component residual profiles calculated from the Jimsphere profile of 28 July 1965 (2259 Z) at Cape Kennedy is illustrated in Figure 5.

B. Definition of Gust

The definition of gust used in this study satisfies the objective to provide data that are suitable for a detailed statistical analysis of singularities and quasi-sinusoidal perturbations that are often observed in Jimsphere wind profiles. A statistical model of these gusts so defined will be developed that will be useful for certain types of flight simulations of space vehicle ascent through the perturbed atmosphere.

According to the conventional approach, a gust profile is calculated by applying a high-pass digital filter to a Jimsphere profile; all the magnitudes in the filtered profile are defined as gusts. In this study, these magnitudes are defined as residuals; the maximum positive or negative residual in the vicinity of a specified reference altitude is defined as a gust. A formal definition of gust is given below.

Let u' represent the zonal wind component at a specified reference altitude, H_o, in a residual profile. The zonal gust is defined as the maximum value of u' in the vicinity of altitude H_o with like sign to u' at H_o. The altitude interval associated with the gust is defined as the gust length, L, which is calculated by taking the altitude difference of the zero crossings on either side of the gust; i.e.,

$$L = H_2 - H_1 \tag{7}$$

Table 1. Filter Design Parameters, Filter Weighting Functions of Four Filters Used for Calculation of Residual Profiles, and Altitude Range of Residual Profiles

Filter Design Parameters

Filter	T(m)	N	$f_c(m^{-1})$	$f_t(m^{-1})$
I	25	20	.00034	.00435
II	250	5	.00004	.00080
III	25	50	.00050	.00150
IV	250	10	0	.000342

Filter Weights

	I	II	III	IV
h_0	0.116360050	0.203331671	0.050406609	0.084765087
.	0.112681533	0.182602840	0.050170253	0.083178582
.	0.102183235	0.130080937	0.049465762	0.078561135
.	0.086369542	0.068650095	0.048306755	0.071321355
h_1	0.067415386	0.020649325	0.046715542	0.062084219
.	0.047750214	-0.003649032	0.044722562	0.051615690
.	0.029618173		0.042365613	0.040733073
.	0.014711243		0.039688904	0.030213801
.	0.003949048	1.000000000	0.036741958	0.020715102
.	-0.002560992		0.033578388	0.012714788
.	-0.005394941		0.030254595	0.006479712
.	-0.005565475		0.026828417	
.	-0.004229394		0.023357771	
.	-0.002423366		0.019899321	1.000000000
.	-0.000884042		0.016507215	
.	0.000021198		0.013231923	
.	0.000259004		0.010119200	
.	0.000022211		0.007209211	
.	-0.000405784		0.004535825	
.	-0.000771288		0.002126107	
h_N	-0.000925530		0.000000000	
			-0.001829786	
			-0.003357689	
			-0.004585029	
			-0.005519564	
			-0.006174897	
			-0.006569761	
			-0.006727193	
			-0.006673649	
			-0.006438065	
			-0.006050919	
			-0.005543301	
			-0.004946033	
			-0.004288852	
			-0.003599693	
			-0.002904062	
			-0.002224550	
			-0.001580449	
			-0.000987520	
			-0.000457877	
			.333639299-12	
			0.000381141	
			0.000683858	
			0.000909429	
			0.001061717	
			0.001146732	
			0.001172171	
			0.001146932	
			0.001080646	
			0.000983218	
			0.000864417	
$h_0 + 2\sum_1^N h_i$	1.000000001		0.999999999	

Altitude Range of Residual Profiles

Filter	Z_{min} (km)	Z_{max} (km)
I	0.5	19.50
II	1.75	18.25
III	1.25	18.75
IV	3.75	16.25

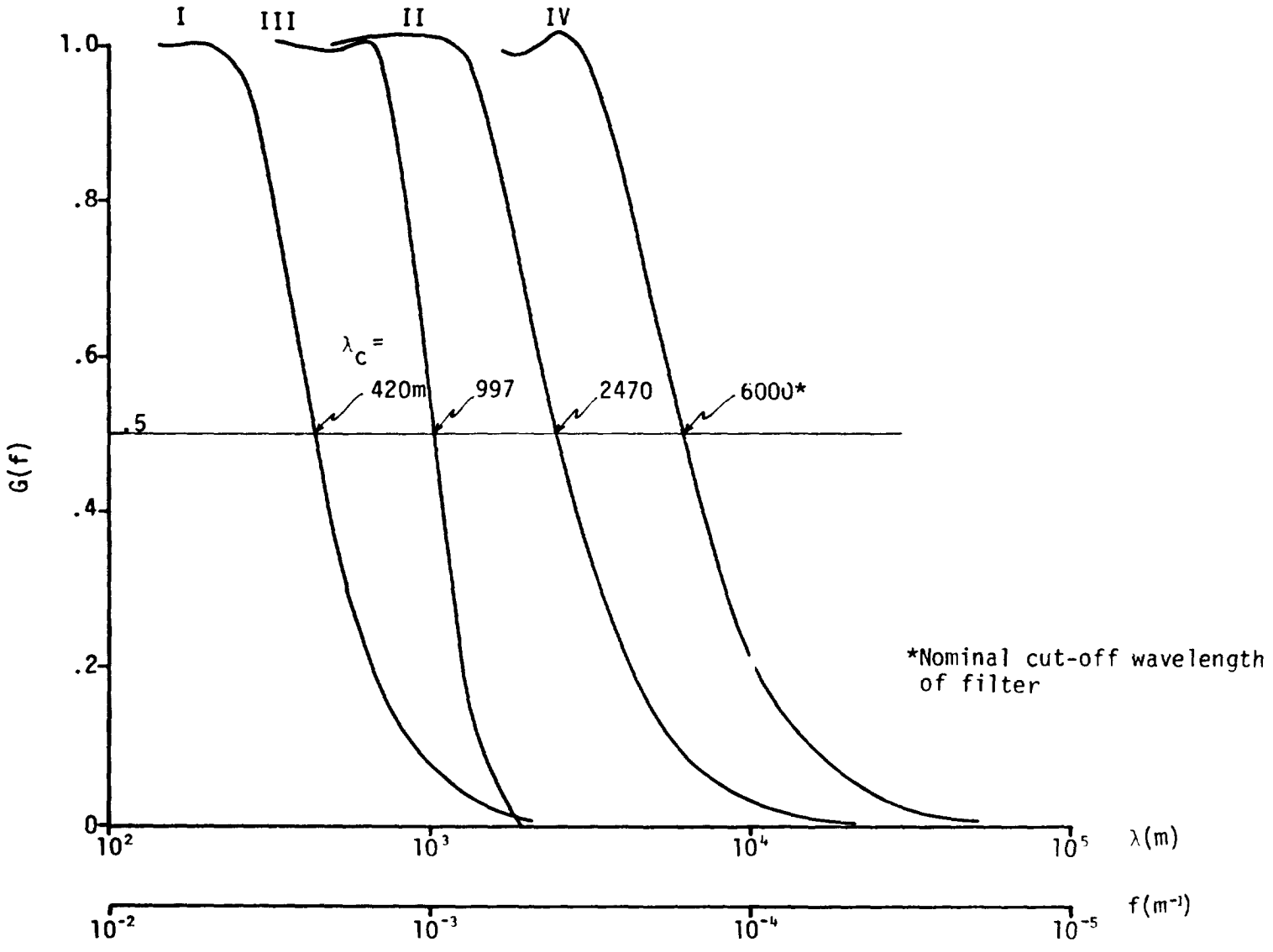

Figure 4. Amplitude Response of Four Digital Filters Used for Calculation of Residual Profiles

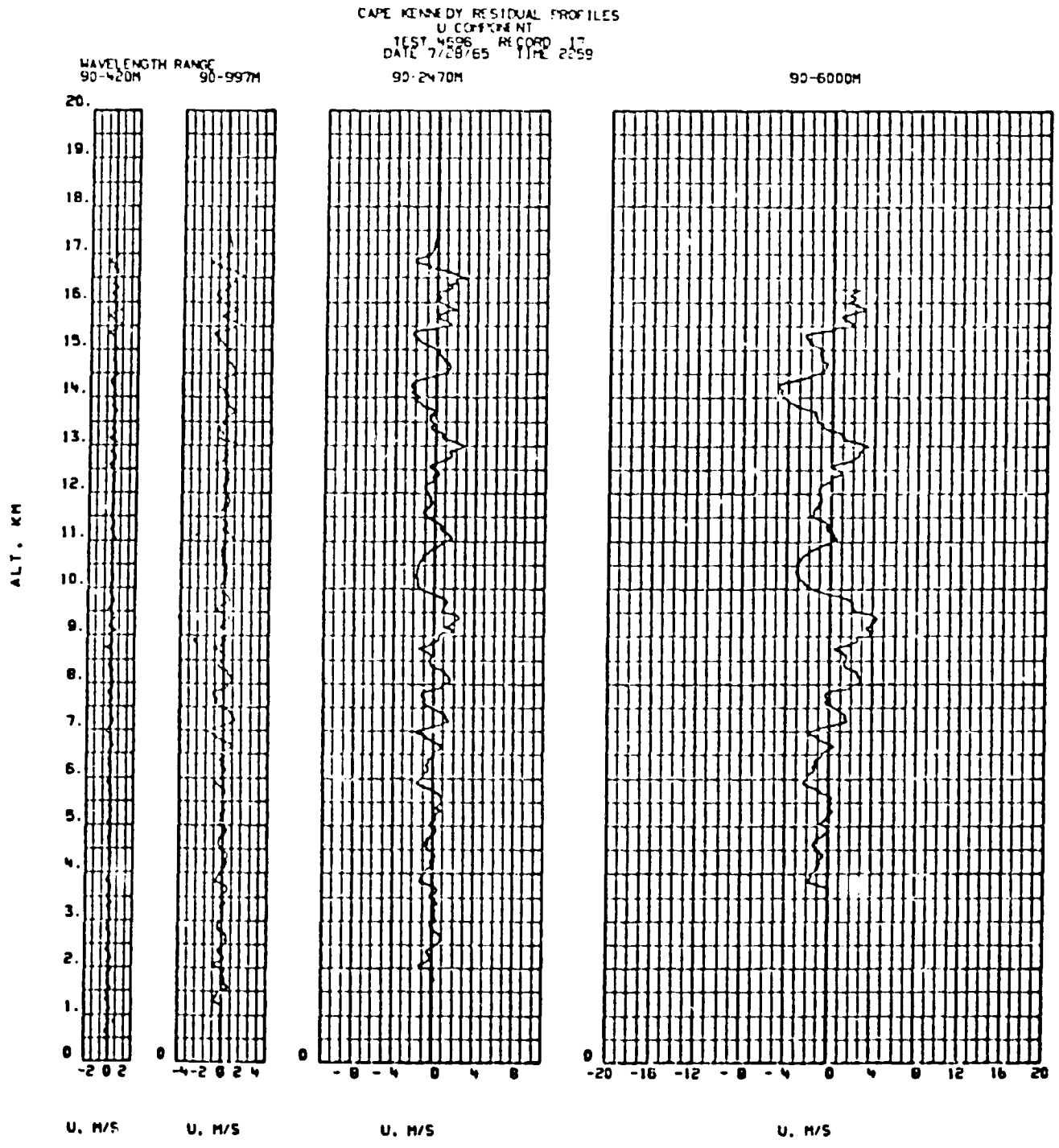

Figure 5. Cape Kennedy Residual Profiles

The altitudes of the zero crossings, H_2 and H_1, are calculated by linear interpolation according to

$$H_2 = H_{j-1} - \frac{25}{u'_j - u'_{j-1}} u'_{j-1} \tag{8}$$

$$H_1 = H_{k+1} - \frac{25}{u'_{k+1} - u'_k} u'_{k+1} \tag{9}$$

where

H_2 = altitude of the first zero crossing for the upward scan

u'_{j-1} = last value of u' with the like sign of u' at H_0 when scanning upward[1]

u'_j = first value of u' with sign opposite to sign of u' at H_0 when scanning downward

H_{j-1} = altitude of u'_{j-1}

H_1 = altitude of the first zero crossing for the downward scan

u'_{k+1} = last value of u' with like sign to sign of u' at H_0 when scanning downward

u'_k = first value of u' with sign opposite of u' at H_0 when scanning downward

H_{k+1} = altitude of u'_{k+1}

Similarly, the meridional gust component, v', is defined by substitution of v' for u' above. In most instances, the zonal and meridional component gusts defined in this manner do not occur at the same altitude. This altitude difference, ΔH, is a measure of the phase difference between the components.

A schematic definition of gust is given in Figure 6.

[1]The indices j and k increase upward.

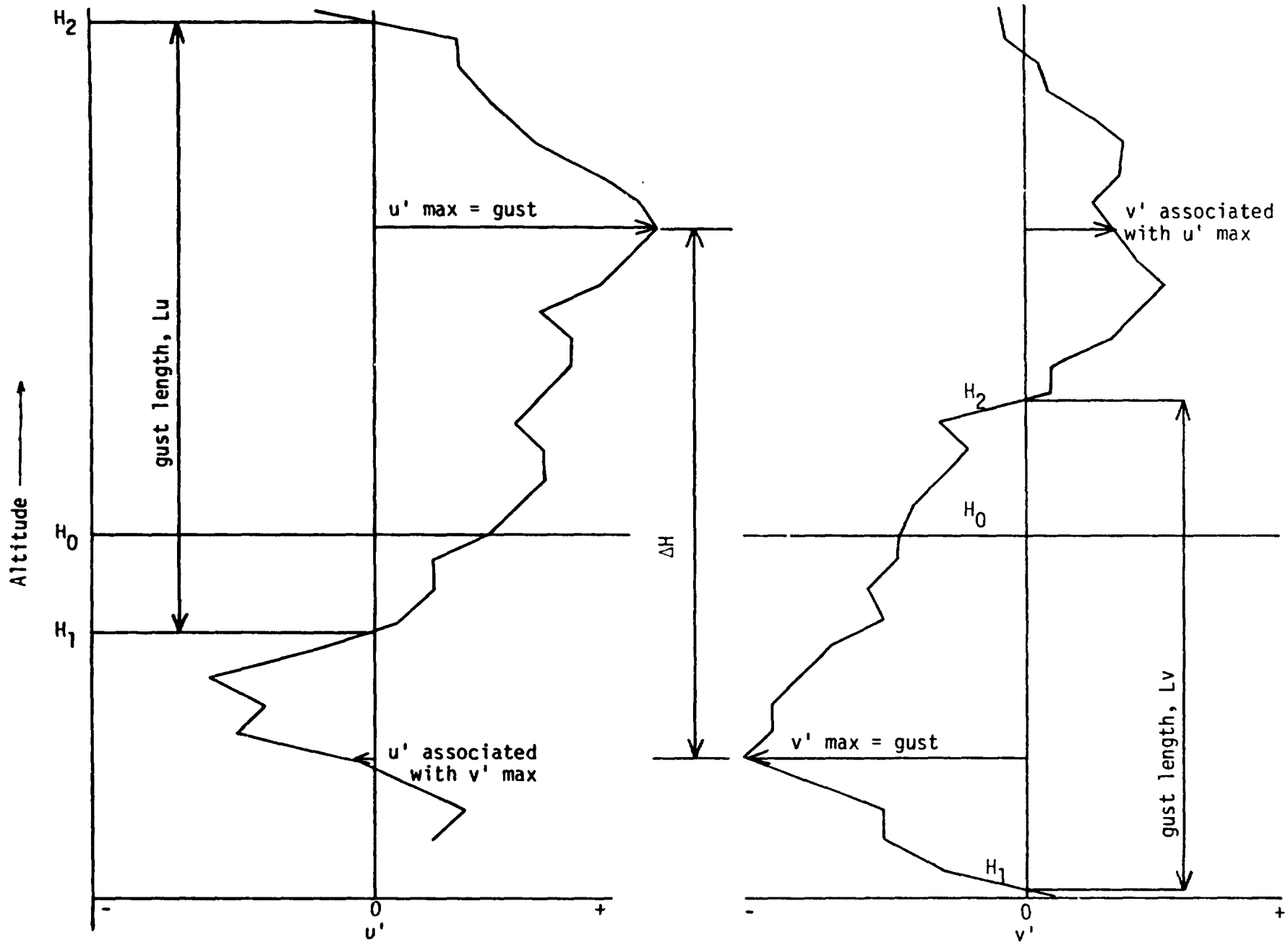

Figure 6. Schematic Definition of Gust

C. Gust Statistical Parameters

The calculation of theoretical gamma distributions of component gust and associated gust length requires that estimates be made of the parameters of the distribution. Methods for estimation of the parameters are described in this section. Examples are presented which illustrate the impact of parameter estimation on the calculated theoretical distributions. Comparisons with observed distributions are presented. The variability of the parameters as a function of altitude and filter cut-off frequency is also described.

1. Parameter Estimation. The parameters of the gamma distribution are estimated from sample statistics. The scaling parameter, β, is calculated from an estimate of the shape parameter, γ, according to

$$\hat{\beta} = \hat{\gamma}/\bar{x} \tag{10}$$

The parameter, γ, can be estimated according to the moments method (M)

$$\hat{\gamma} = (\bar{x}/\sigma)^2 \tag{11}$$

where $\bar{x}$ and σ are the mean and standard deviation of the data sample.

Alternatively, an estimate of γ can be obtained from either of two maximum likelihood procedures; according to Thom (Ref. 7), $\hat{\gamma}$ is given by (MLI)

$$\hat{\gamma} = \frac{1}{4A}\left(1 + \sqrt{1 + 4A/3}\right) \tag{12}$$

where $$A = \ln(\bar{x}) - \overline{\ln(x)} \tag{13}$$

According to Bury (Ref. 8), $\hat{\gamma}$ is calculated from a polynomial approximation (MLII) of the form

$$\hat{\gamma} = 1/A\ (.5001 + .1649A - .0544A^2) \qquad (14)$$

for $0 \leq A \leq .577$

and

$$\hat{\gamma} = \frac{8.899 + 9.060A + .977A^2}{A(17.80 + 11.97A + A^2)} \qquad (15)$$

for $.577 \leq A \leq 17$

As illustrated in Figure 7, there is no significant difference between the two ML methods for $A < 1$. The calculated values of parameter A listed in Table 2 are all less than 0.4; therefore, either ML method would be appropriate for estimation of γ from the sample data used in this study. For large sample size ($m >> 20$) and $\gamma < 4$, which characterizes this data sample, the ML method is favored over the moments method (Ref. 9).

Comparisons of observed and theoretical distributions of gust and gust length are illustrated in Figures 8 through 11. The distributions based on ML have smaller values of the shape parameter, γ; these distributions are more skewed than those based on M statistics and deviate more from the observed distributions at the extreme percentiles.

2. Variability of Gamma Distribution Parameters. Variability of the estimates of parameters γ and β is an indication of the variability of the theoretical gust distribution. As indicated earlier, γ determines the shape of the distribution function and β is a scaling parameter. Gust percentiles are inversely related to β, or directly related to β^*, where $\beta^* = 1/\beta$.

The variability of γ and β^* as a function of filter cutoff wavelength, γ_c, and altitude is illustrated in Figures 12 and 13 for u component gust and in Figures 14 and 15 for v component gust. The parameters were estimated by the moments method; the variability is similar for estimates based on the method of maximum likelihood. As illustrated in Figures 12 and 14, the value of γ is usually between 2.25 and 3.70 for both components; the variability within that range is not

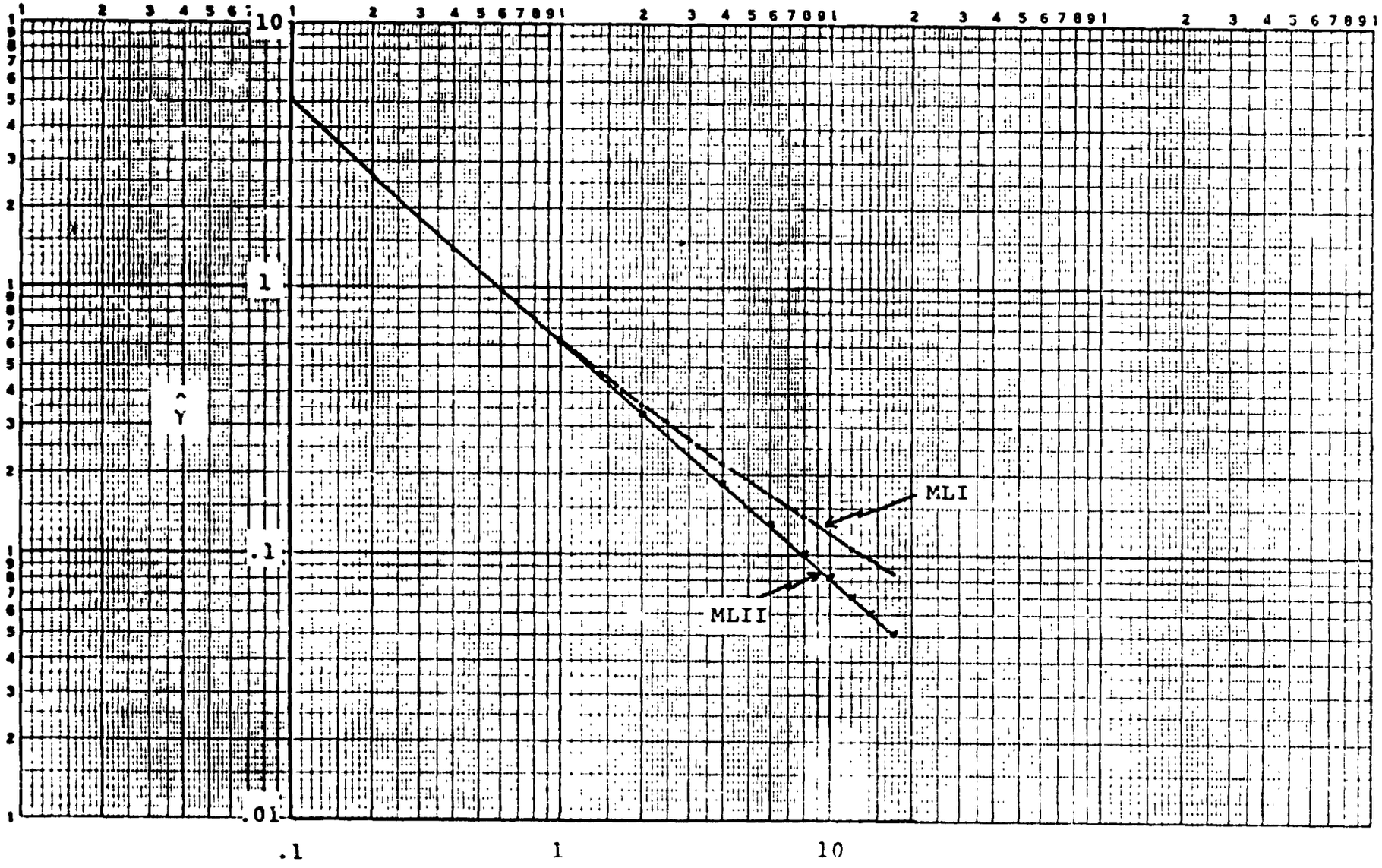

Figure 7. Maximum Likelihood Estimates of γ Based on Thom (MLI, Ref. 7) and Bury (MLII, Ref. 8). Parameter, A, is Calculated According to Equation 13.

Table 2. Parameter, A, Calculated from Filtered Jimsphere Data during February at Cape Kennedy, Florida

	Altitude (km)	4	6	8	10	12	14
λ_c = 420m	|u'|	.2454	.2912	.2575	.2030	.2764	.3379
	|v'|	.2421	.2245	.2453	.2285	.2557	.2900
	LU	.1564	.1514	.1922	.1308	.2193	.2117
	Lv	.1444	.1850	.1653	.1802	.2199	.1783
λ_c = 997m	|u'|	.1850	.2745	.2541	.1973	.2169	.2879
	|v'|	.1989	.2349	.2297	.2889	.2057	.2487
	LU	.1367	.1977	.1818	.2059	.2298	.2697
	Lv	.1326	.1550	.2061	.2893	.2462	.2603
λ_c = 2470m	|u'|	.2009	.2068	.2396	.2072	.3120	.2322
	|v'|	.1875	.2083	.2828	.2187	.2601	.2804
	LU	.2145	.1958	.2625	.2401	.2807	.2903
	Lv	.1929	.1849	.2768	.2330	.3759	.3334
λ_c = 6000m	|u'|	*	.2970	.2453	.2621	.2956	.2040
	|v'|	*	.2170	.3479	.2920	.2943	.2413
	LU	*	.3436	.3263	.2851	.3647	.3198
	Lv	*	.1993	.3370	.2994	.3710	.3646

*Insufficient data

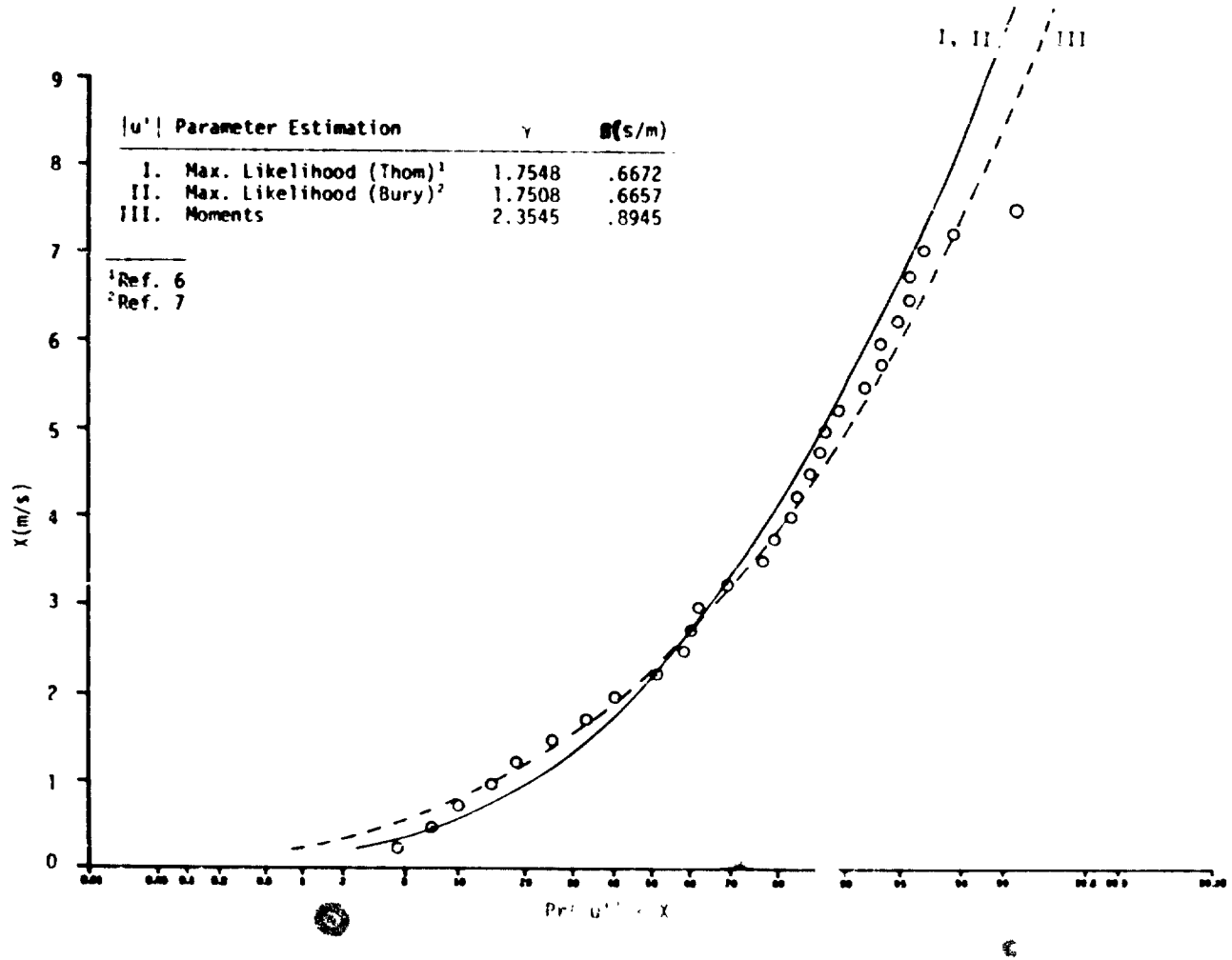

Figure 8. Observed (Plotted Points) and Theoretical Distributions (Curves I, II, and III) of u Component Gust at 12 km During February at Cape Kennedy, Florida, for λ_c = 2470 m

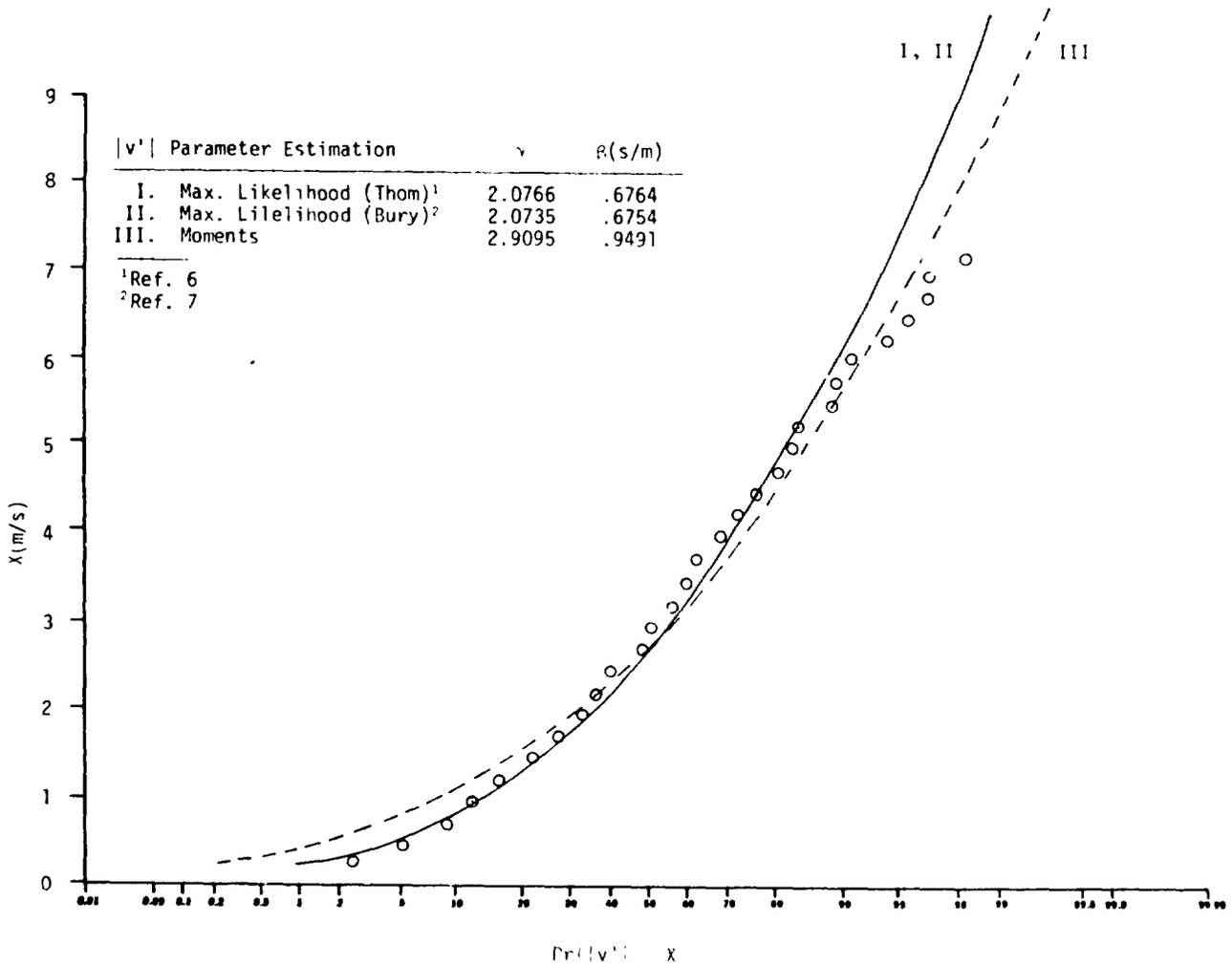

Figure 9. Observed (Plotted Points) and Theoretical Distributions (Curves I, II, and III) of v Component Gust at 12 km During February at Cape Kennedy, Florida, for λ_c = 2470 m

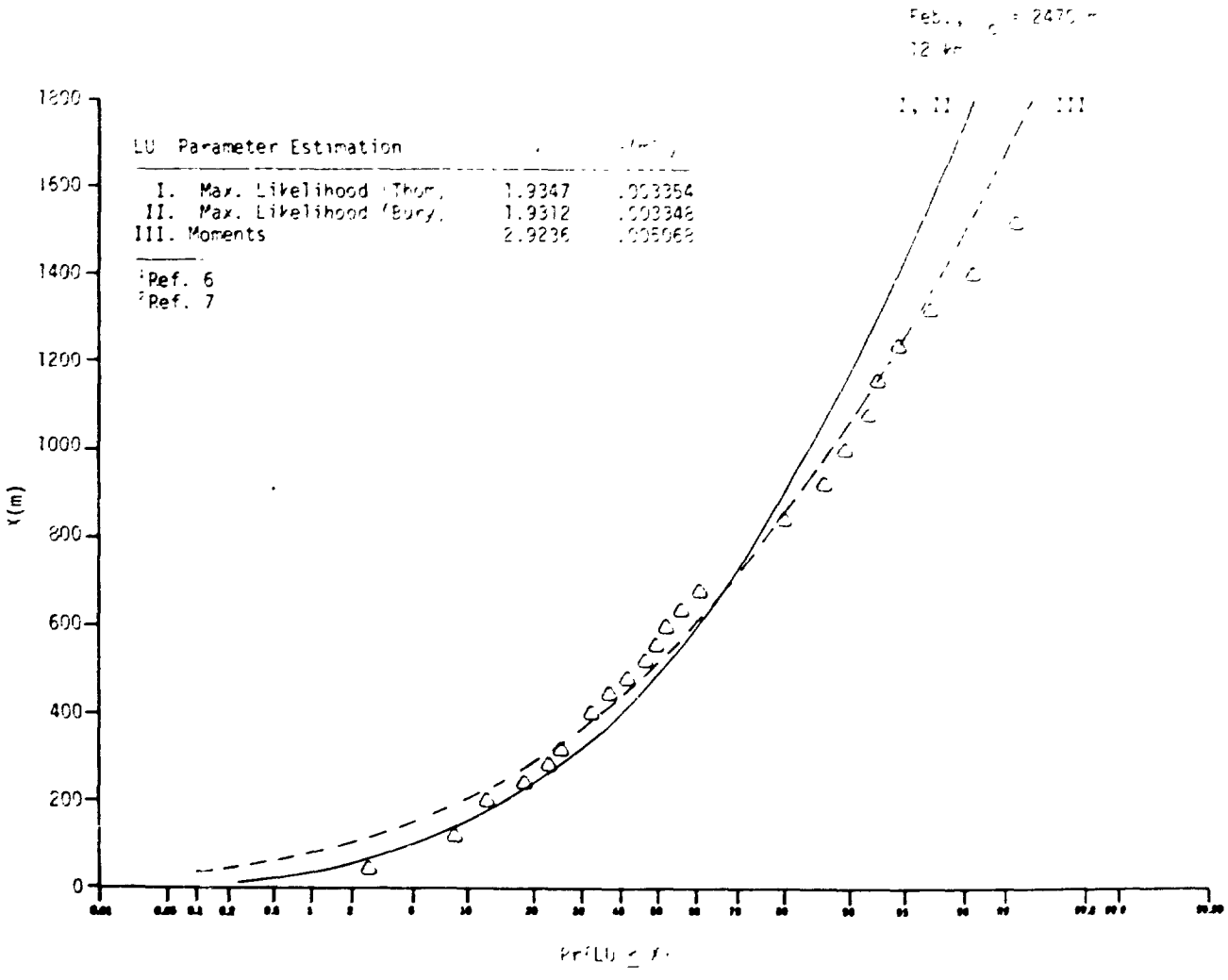

Figure 10. Observed (Plotted Points) and Theoretical Distributions (Curves I, II, and III) of u Component Gust Length, LU, at 12 km During February at Cape Kennedy, Florida, for λ_c = 2470 m

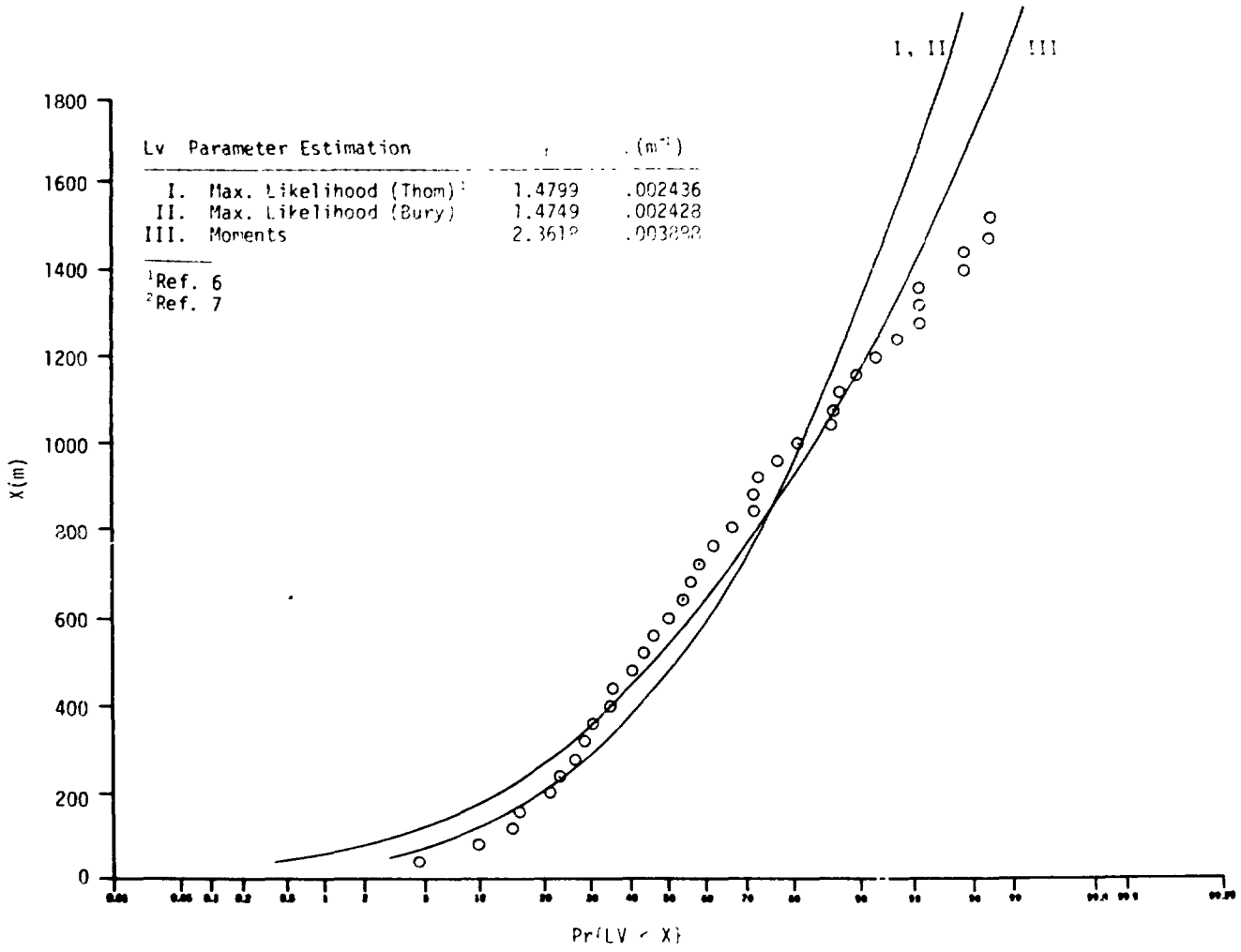

Figure 11. Observed (Plotted Points) and Theoretical Distributions (Curves I, II, and III) of v Component Gust Length, Lv, at 12 km During February at Cape Kennedy, Florida, for λ_c = 2470 m

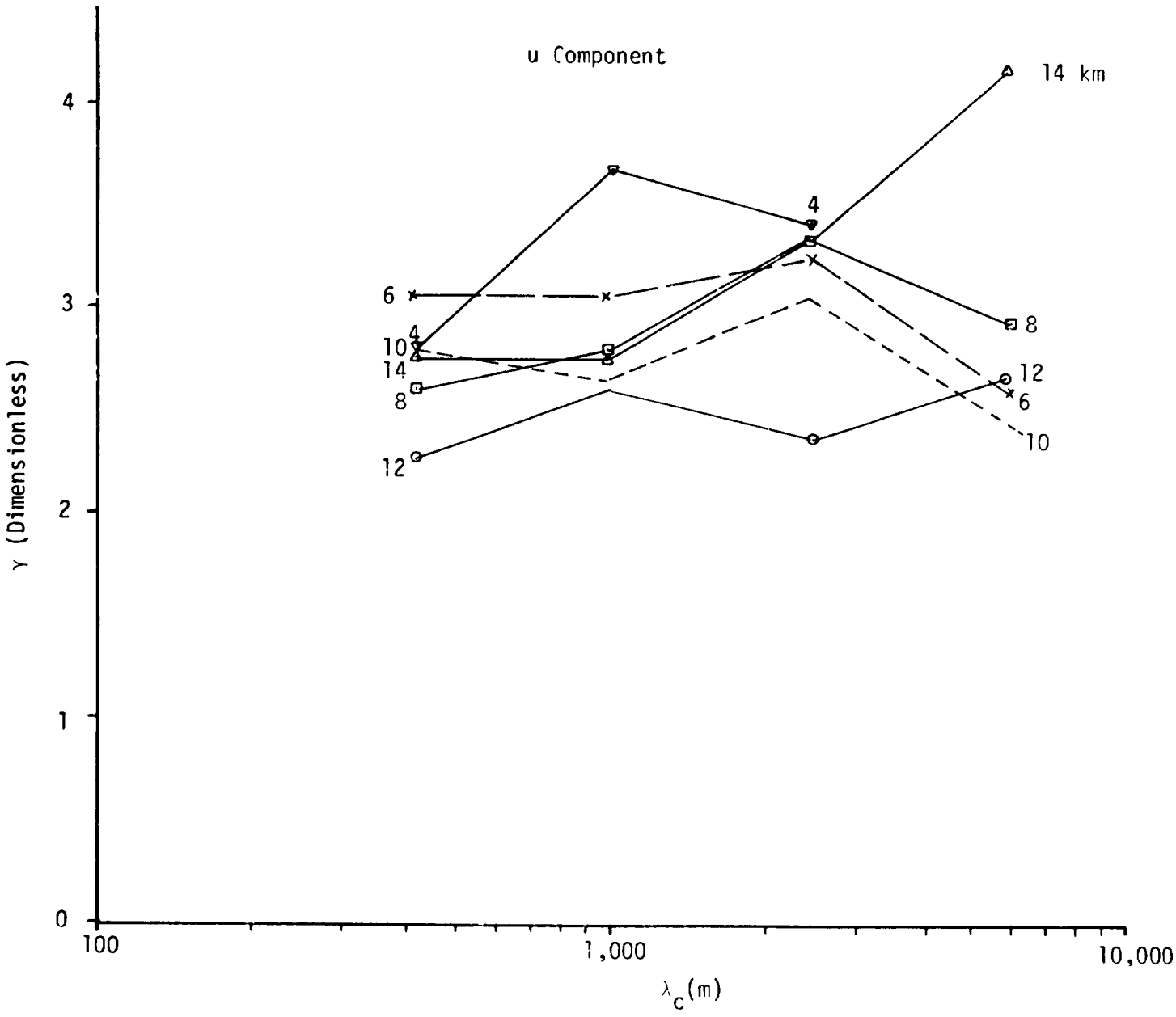

Figure 12. Parameter γ of the Gamma Distribution of Zonal Component Gust During February at Cape Kennedy as a Function of Filter Cut-off Frequency, λ_c, and Altitude

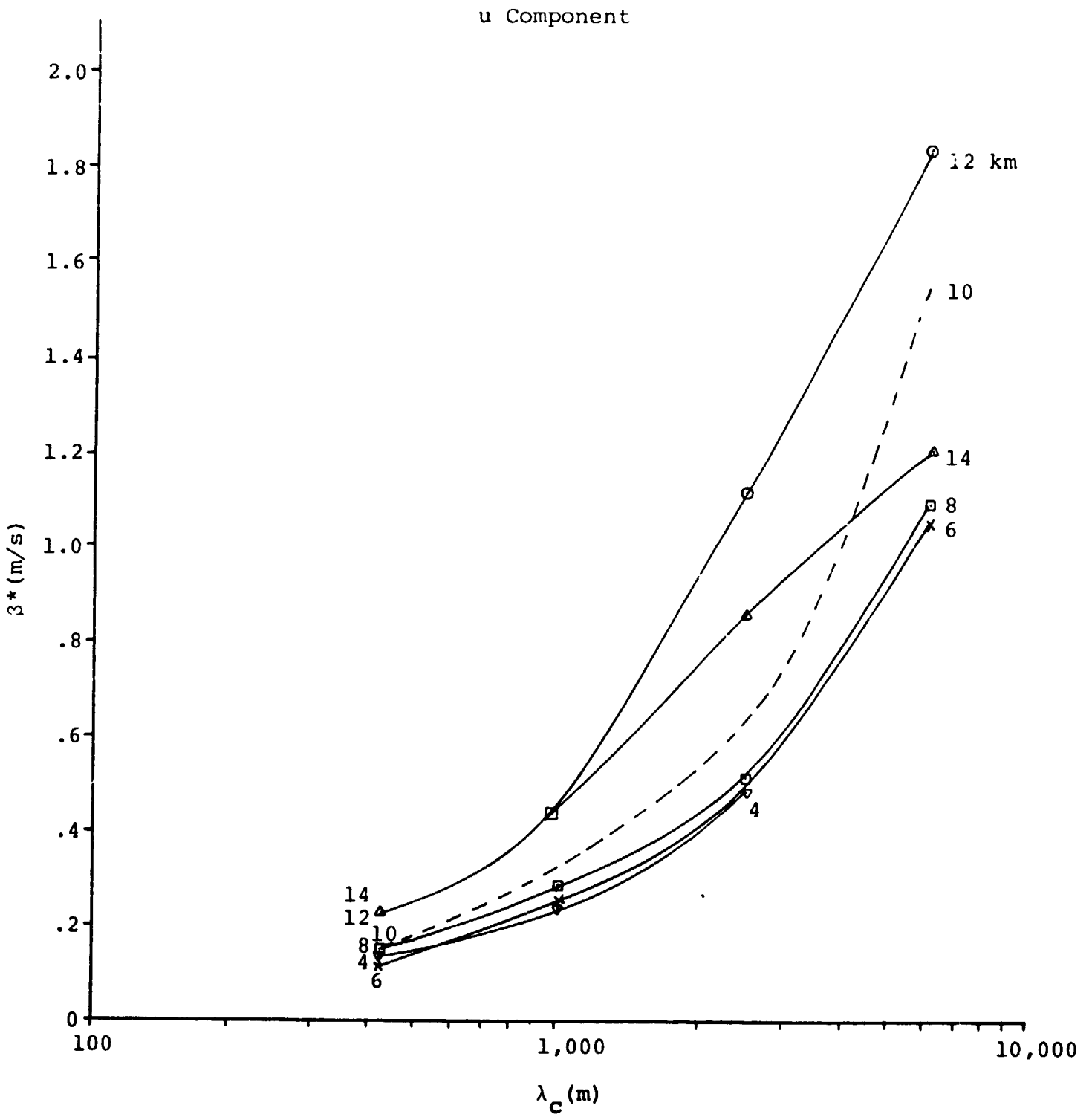

Figure 13. Parameter β* of the Gamma Distribution of Zonal Component Gust During February at Cape Kennedy as a Function of Filter Cut-off Frequency, λ_c, and Altitude

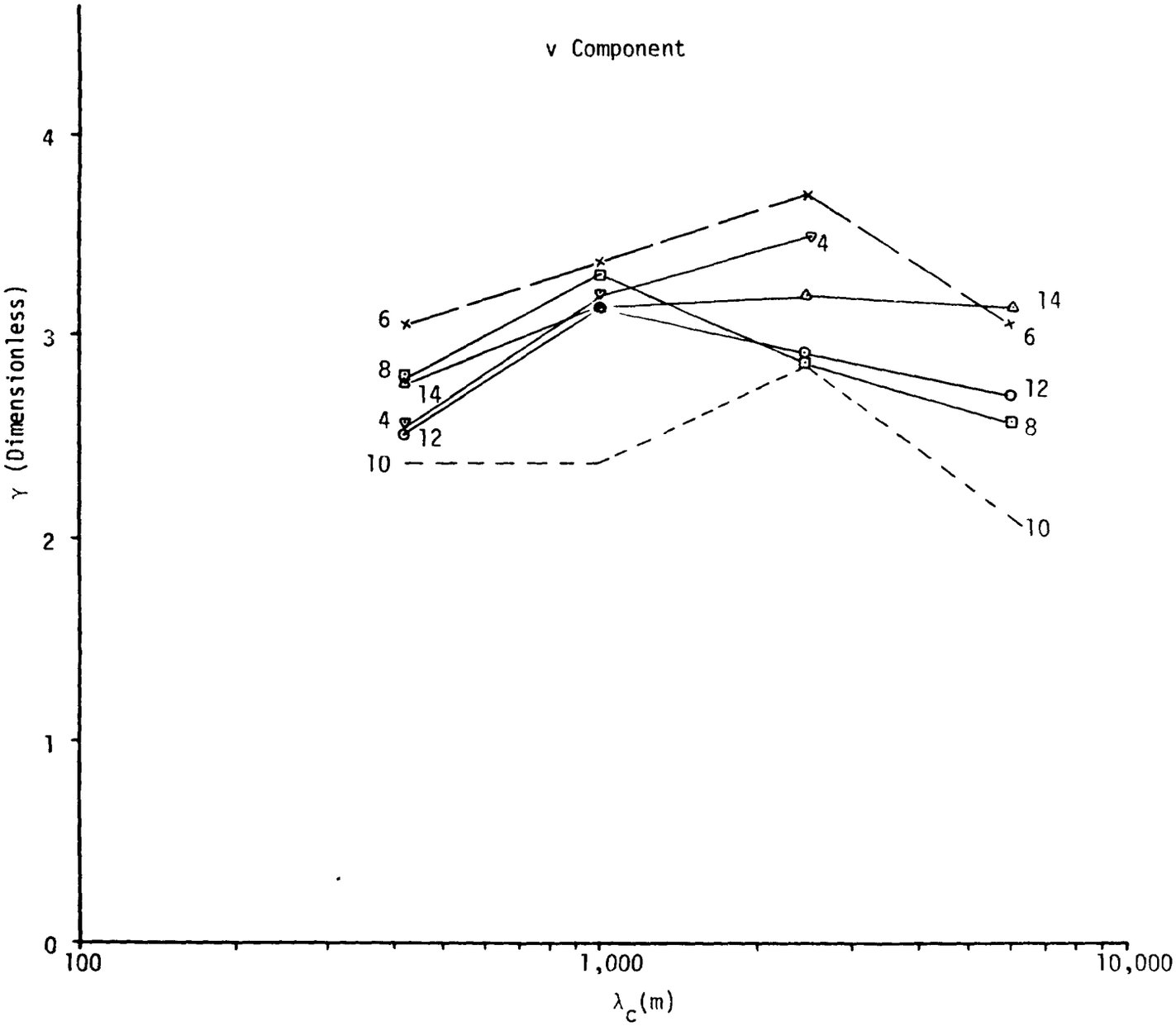

Figure 14. Parameter γ of the Gamma Distribution of Meridional Component Gust During February at Cape Kennedy as a Function of Filter Cut-off Frequency, λ_c, and Altitude

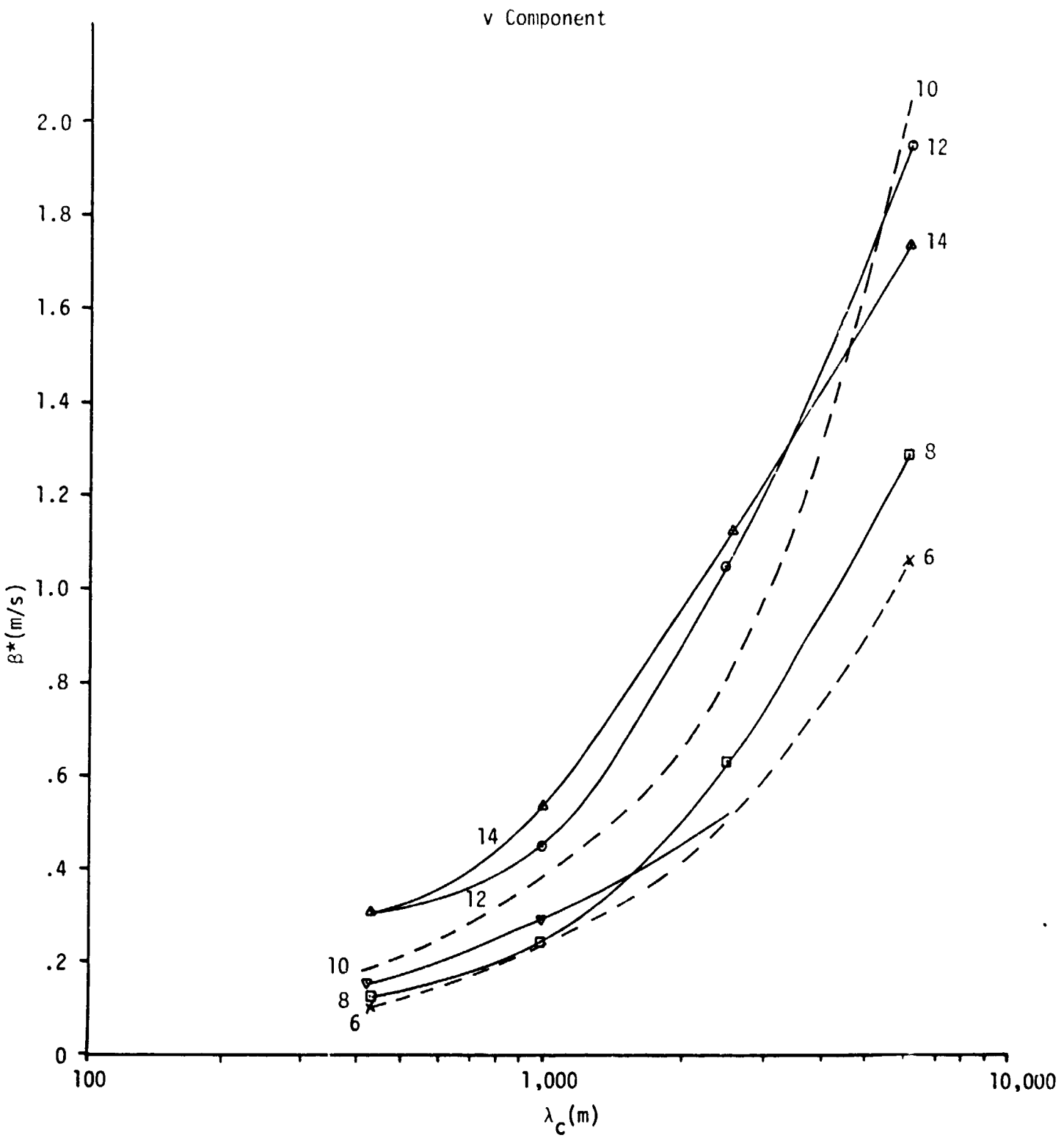

Figure 15. Parameter β* of the Gamma Distribution of Meridional Component Gust During February at Cape Kennedy as a Function of Filter Cut-off Frequency, λ_c, and Altitude

clearly systematic with respect to either altitude or filter cut-off frequency. As illustrated in Figures 13 and 15, the scaling parameter, β^*, is strongly influenced by filter cut-off frequency and, to a somewhat lesser extent, by altitude; β^* increases as γ_c increases; the increase of β^* with altitude is most pronounced between 8 and 10 km.

D. Gamma Distribution of Gust at Reference Altitudes

1. Univariate Gamma for Gust Components and Associated Gust Lengths. The univariate gamma is calculated from sample estimates of the parameters γ and β. In this section, examples are presented which illustrate the following:

- Comparison of theoretical (gamma) and observed distributions for various filter cut-off wavelengths
- Seasonal variation of theoretical distributions
- Altitude variation of theoretical distributions
- Comparison of zonal and meridional component theoretical distributions.

The parameters used in the theoretical distributions used in the various examples were calculated by the moments method (described in Section III.C.1).

Theoretical and observed distributions at 12 km during February are illustrated in Figures 16 through 19; all the distributions exhibit a similar variation as a function of filter cut-off wavelength, λ_c. No large systematic differences between the observed and theoretical distributions are noted.

The variation of theoretical distributions with season is illustrated in Figures 20 through 23. Three months, February, July, and April, were selected to represent the winter, summer, and transition seasons, respectively, at Cape Kennedy. It is indicated that large seasonal differences for

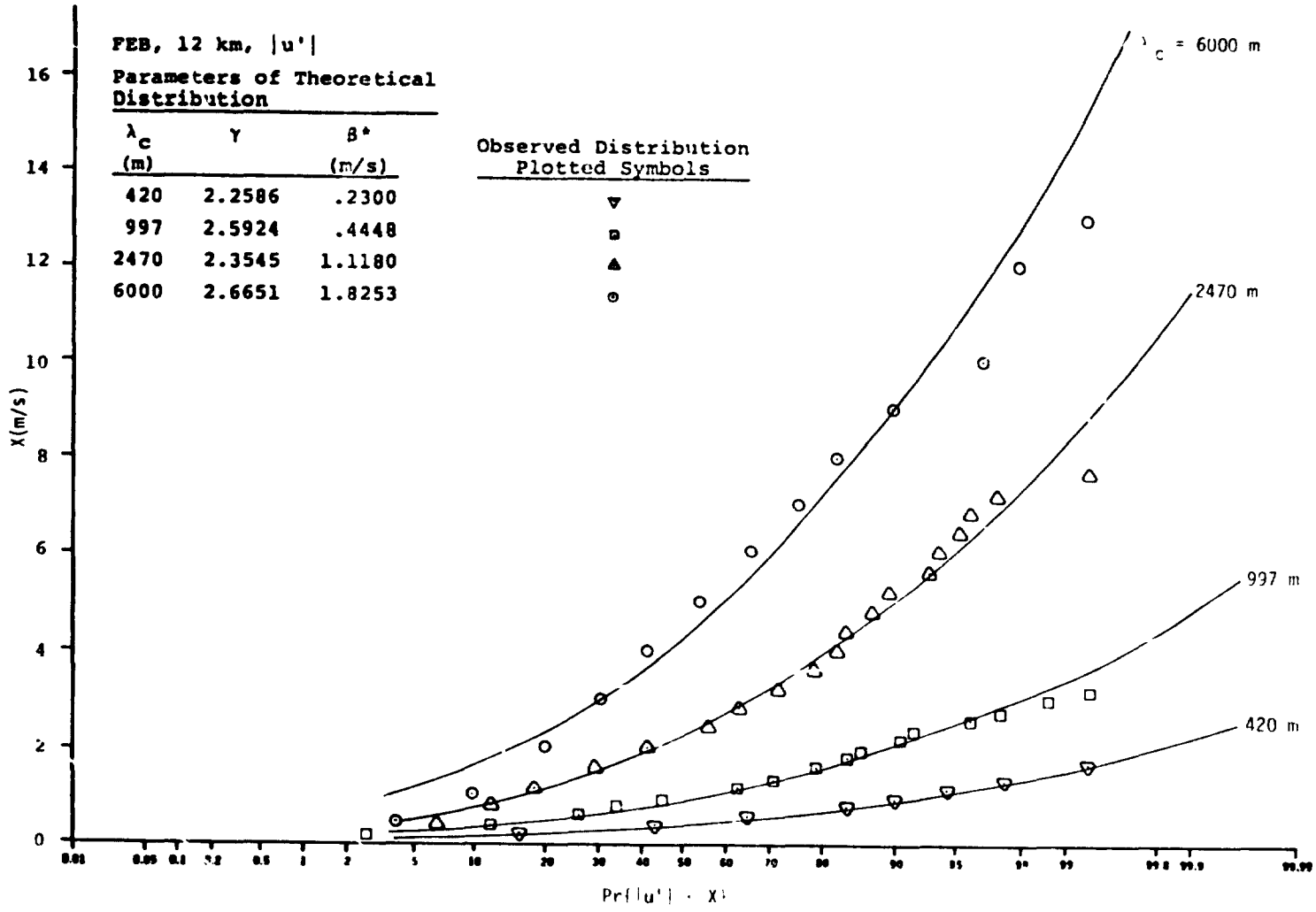

Figure 16. Observed and Theoretical (Gamma) Distribution of Absolute u Component Gust at a Reference Height of 12 km During February at Cape Kennedy as a Function of Filter Cut-off Wavelength, λ_c

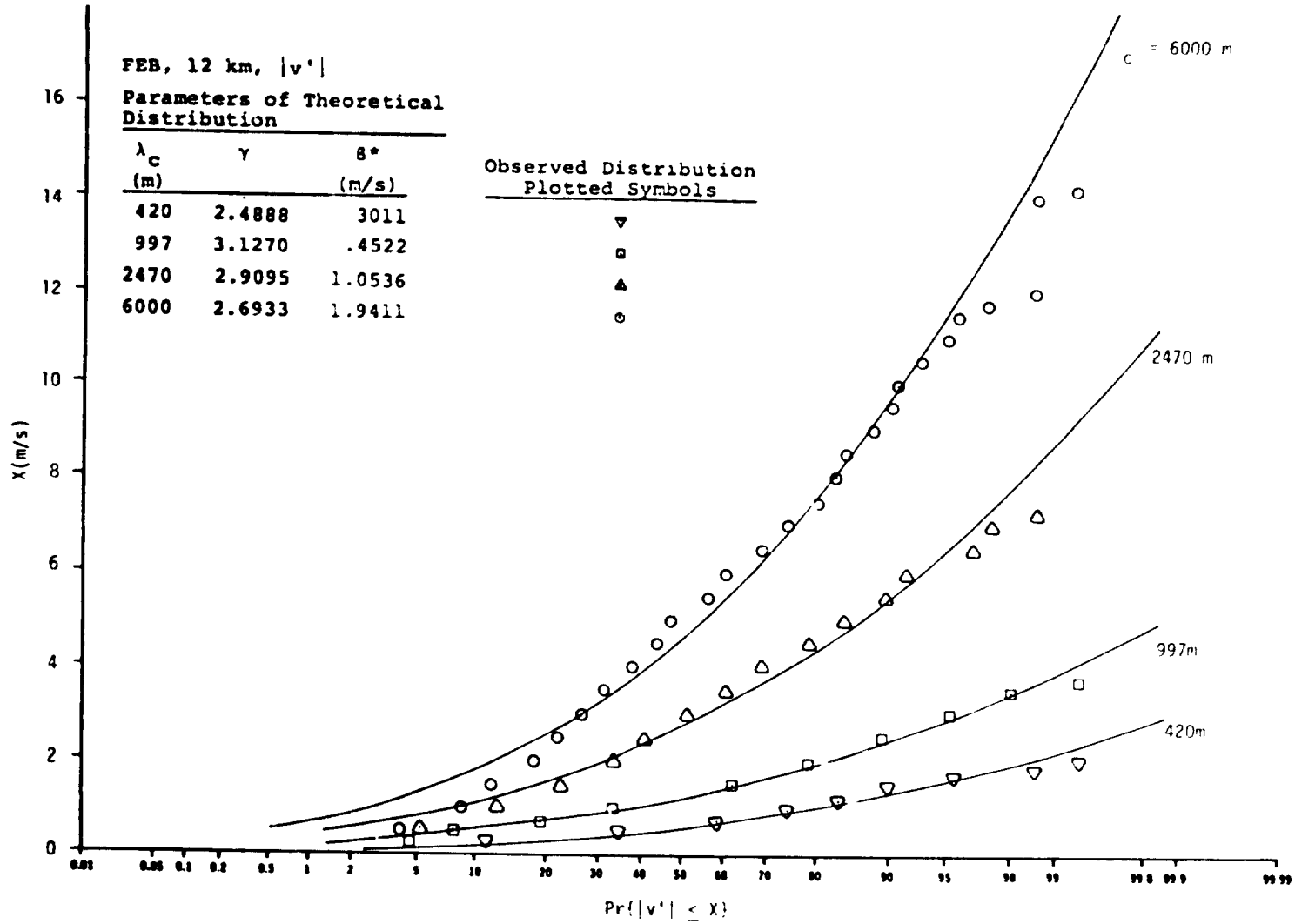

Figure 17. Observed and Theoretical (Gamma) Distribution of Absolute v Component Gust at a Reference Height of 12 km During February at Cape Kennedy as a Function of Filter Cut-off Wavelength, λ_c

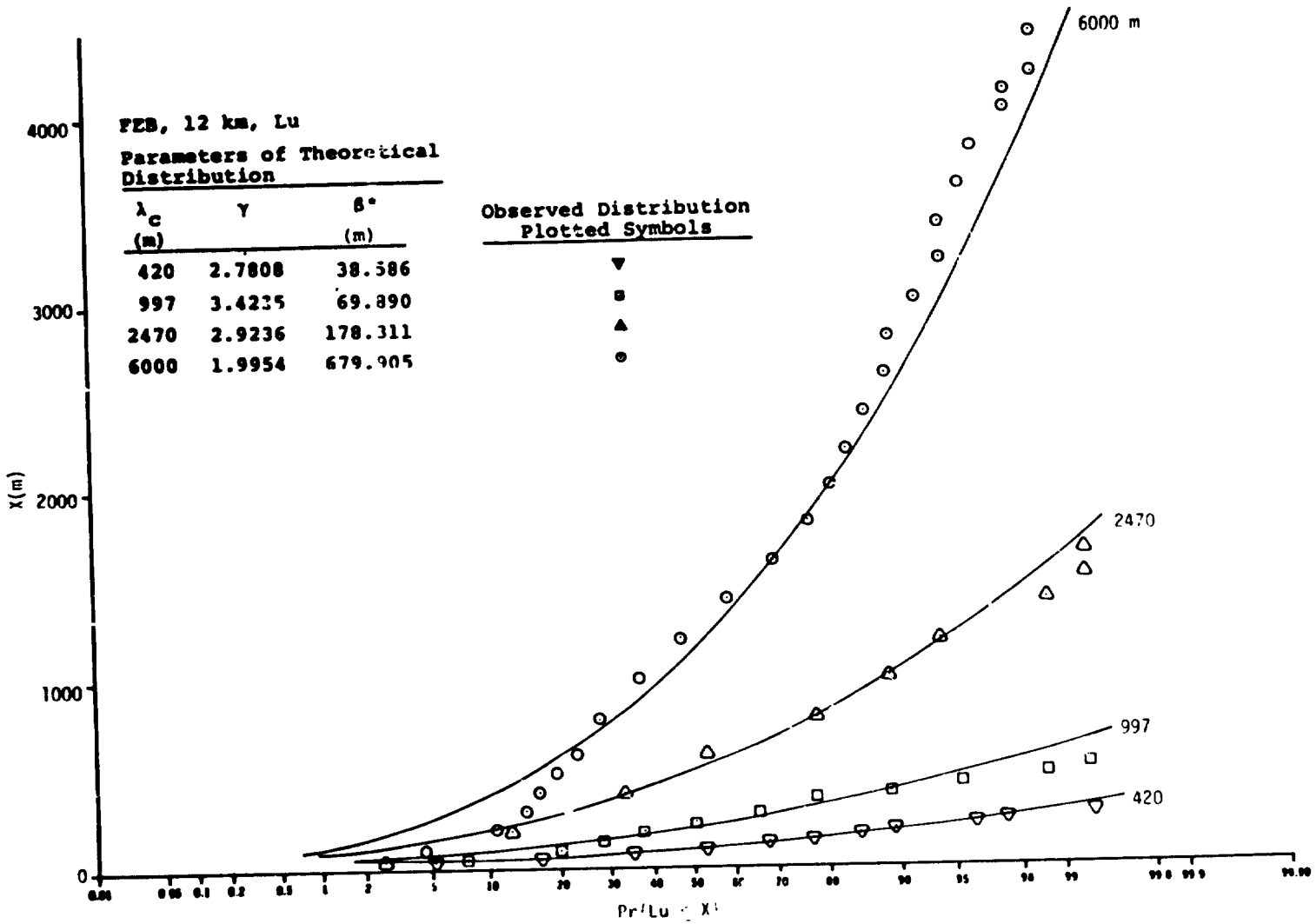

Figure 18. Observed and Theoretical (Gamma) Distribution of u Component Gust Length, Lu, at a Reference Height of 12 km During February at Cape Kennedy as a Function of Filter Cut-off Wavelength, λ_c

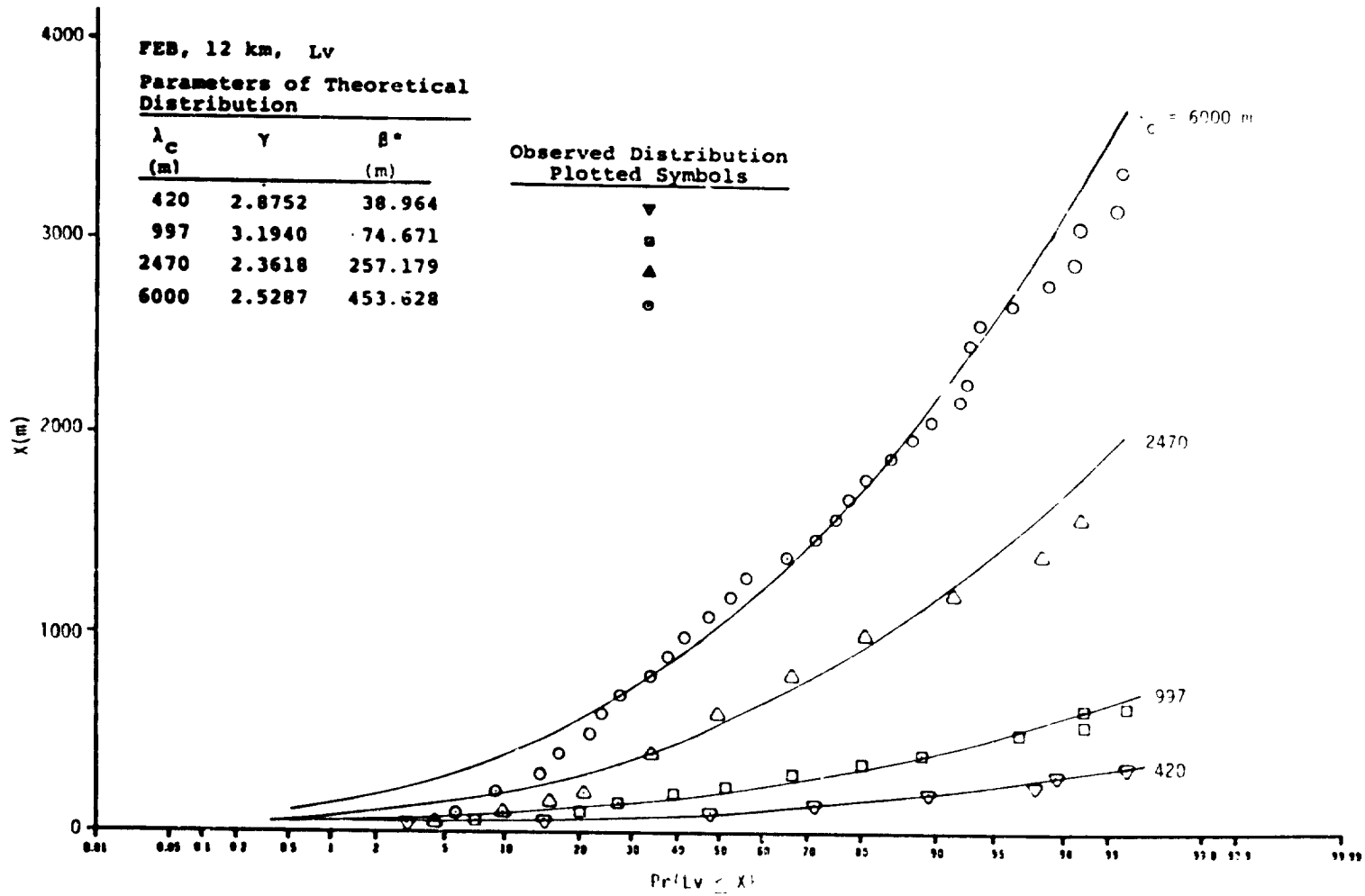

Figure 19. Observed and Theoretical (Gamma) Distribution of v Component Gust Length, Lv, at a Reference Height of 12 km During February at Cape Kennedy as a Function of Filter Cut-off Wavelength, λ_c

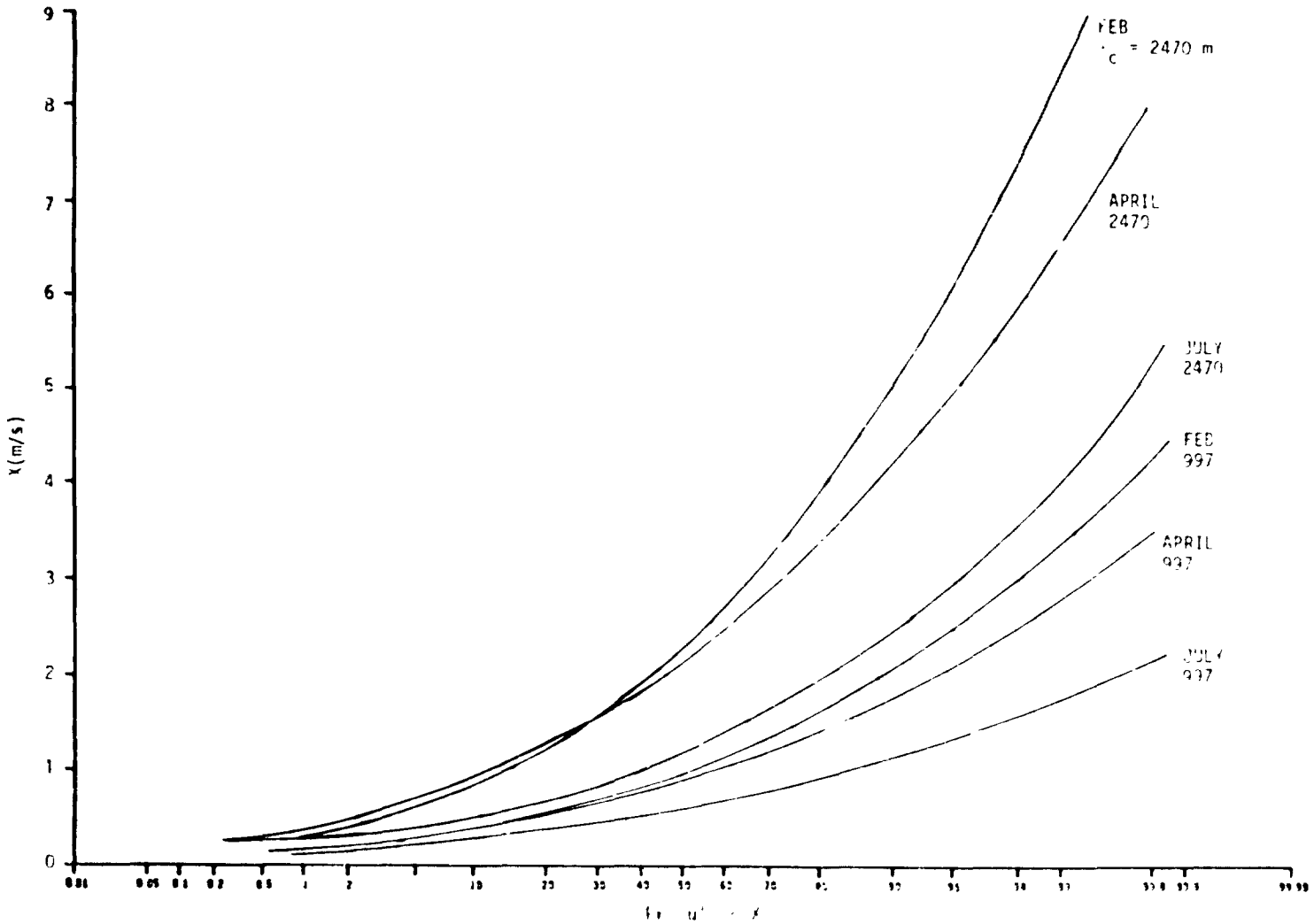

Figure 20. Theoretical Distribution of Absolute u Component Gust at a Reference Height of 12 km During February, April, and July

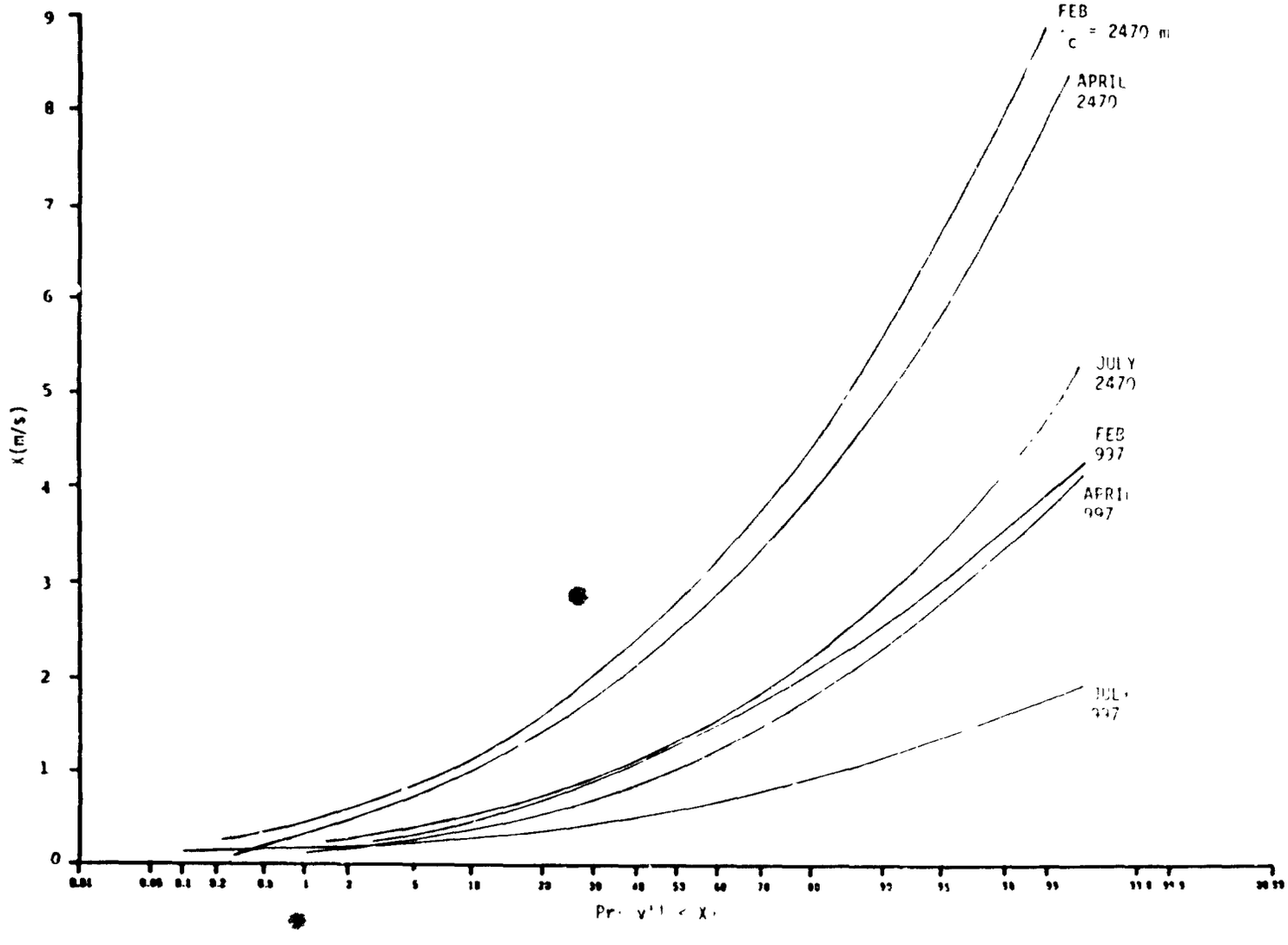

Figure 21. Theoretical Distribution of Absolute v Component Gust at a Reference Height of 12 km During February, April, and July

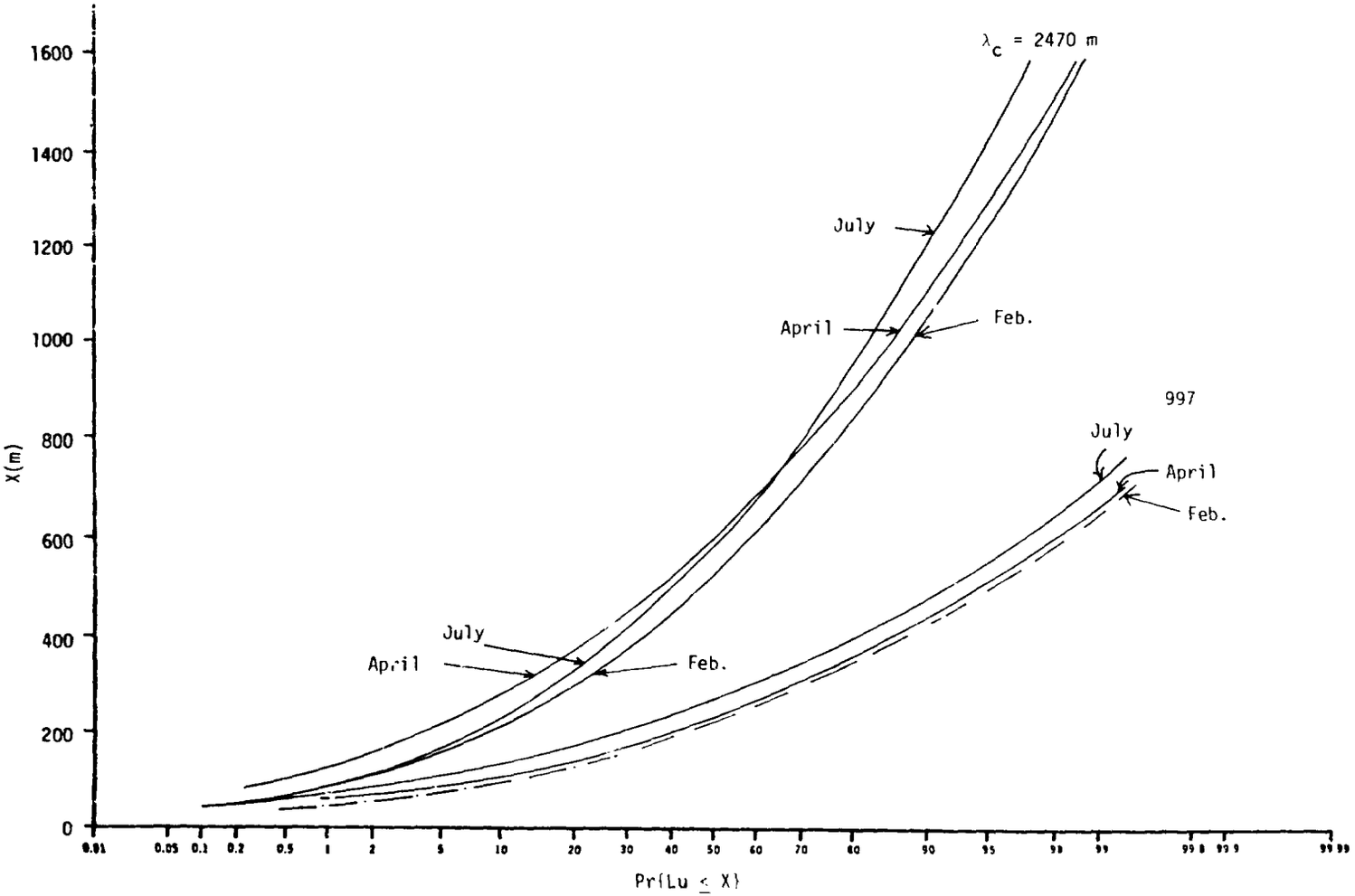

Figure 22. Theoretical Distribution of u Component Gust Length, Lu, at a Reference Height of 12 km During February, April, and July

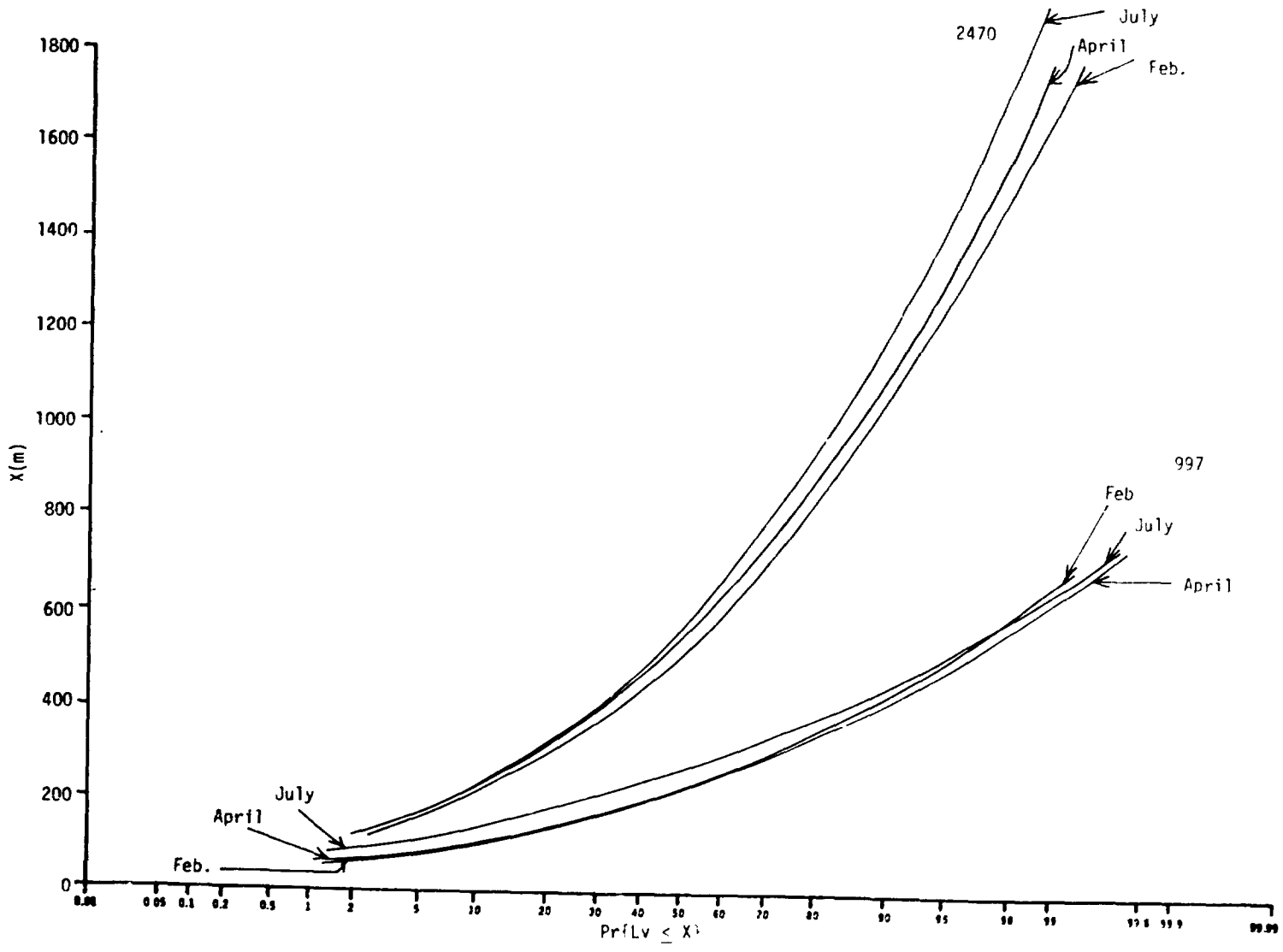

Figure 23. Theoretical Distribution of v Component Gust Length, Lv, at a Reference Height of 12 km During February, April, and July

either u or v component absolute gust are not affected by the choice of filter cut-off wavelength. The small seasonal variation of gust length illustrated in Figures 22 and 23 is probably attributable to the unavoidable inaccuracies in the estimation of distribution parameters from sample statistics; therefore, there is no significant variation of gust length distributions with respect to season.

The variation of the theoretical distributions of u and v component absolute gust with altitude is illustrated in Figures 24 and 25. For each filter cut-off frequency, two reference altitudes were selected to illustrate the maximum variation of the distributions in the 4 to 14 km altitude range. The maximum variation does not necessarily occur between 4 and 14 km. It is indicated that there is a significant variation of absolute u and v component gust with altitude.

A comparison of u and v component absolute gust at 8, 12, and 14 km during February is illustrated in Figures 26 through 28. It is indicated that v component gust is consistently larger than u component gust for most of the filter cut-off wavelengths and altitudes considered.

2. Gust Component Percentiles. For engineering and design applications, it would be desirable to derive an empirical function which accurately describes the variation of particular percentiles as a function of filter cut-off wavelength, λ_c. Such a function should be bounded at 0 for $\lambda_c = 0$ and should approach an asymptotic value for large values of λ_c. A function which has this behavior is of the form:

$$|X'|_p = \frac{\lambda_c}{a\lambda_c + b} \tag{16}$$

where $|X'|_p$, the gust component percentile, is asymptotic to the quantity 1/a and the parameters a and b can be estimated by a least-squares technique utilizing a transformation of variables in Equation (16) to obtain a linear equation of the form

$$T = a + bw \tag{17}$$

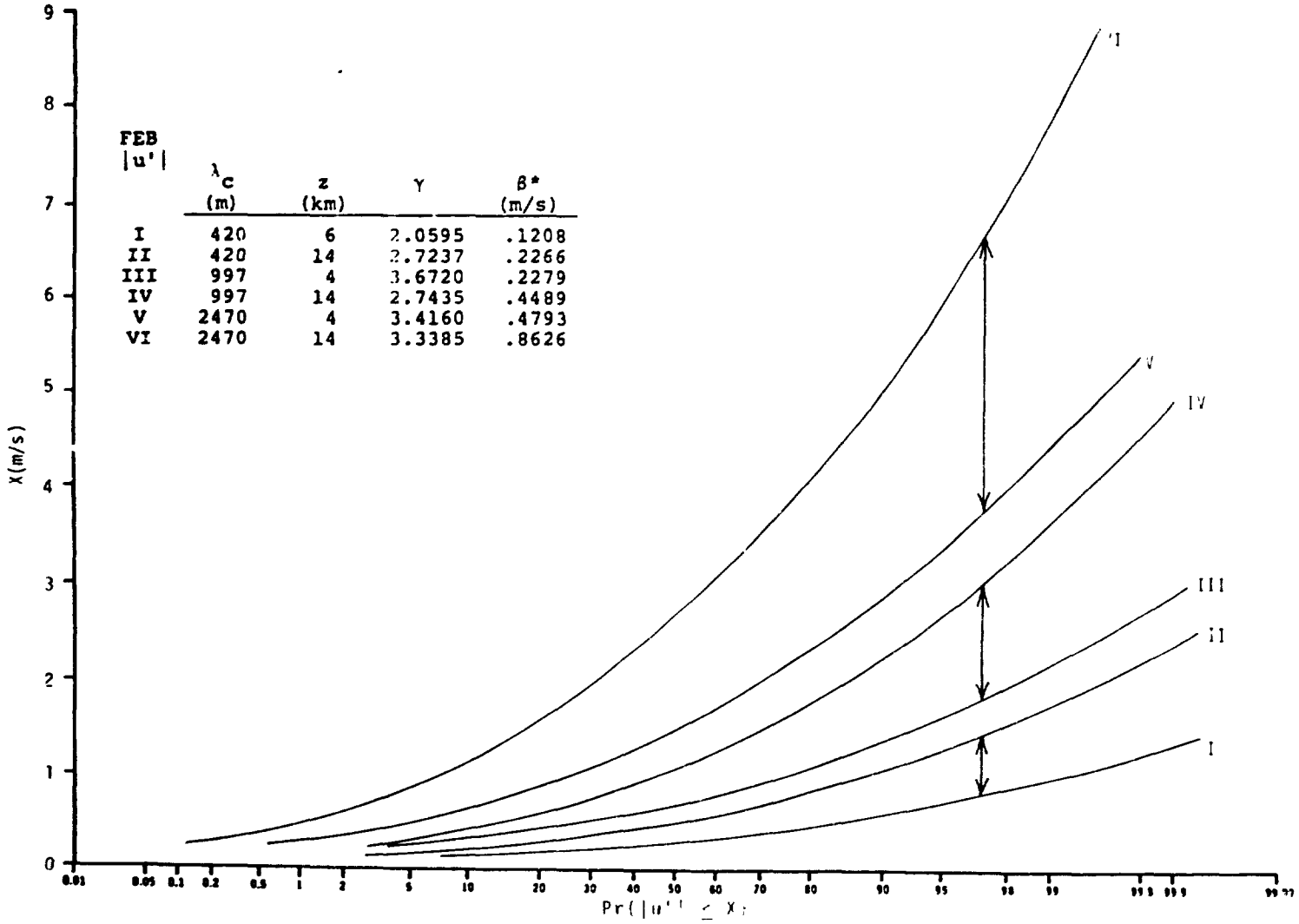

Figure 24. Variability of Theoretical Distribution of Absolute u Component Gust During February at Cape Kennedy as a Function of Altitude

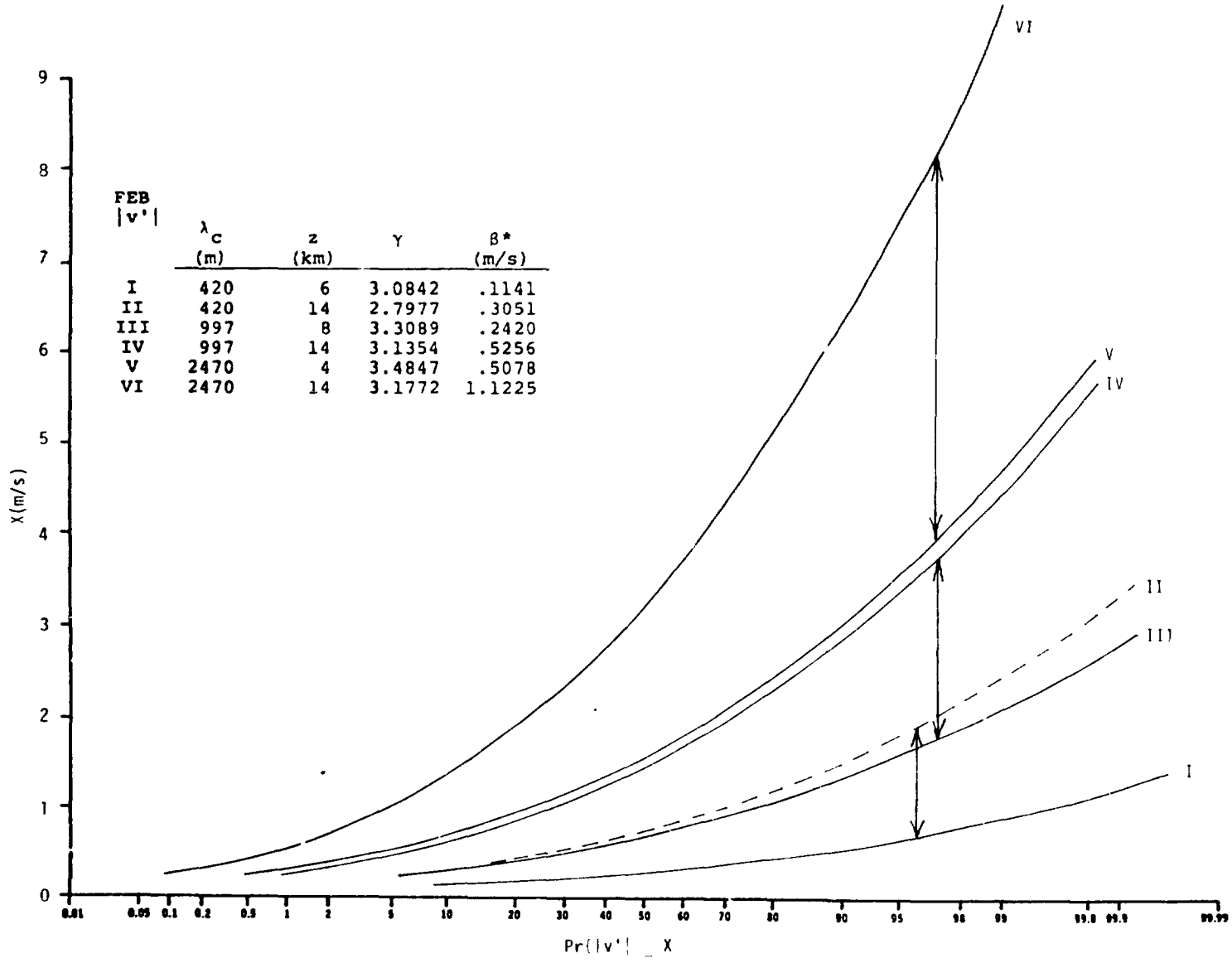

Figure 25. Variability of Theoretical Distribution of Absolute v Component Gust During February at Cape Kennedy as a Function of Altitude

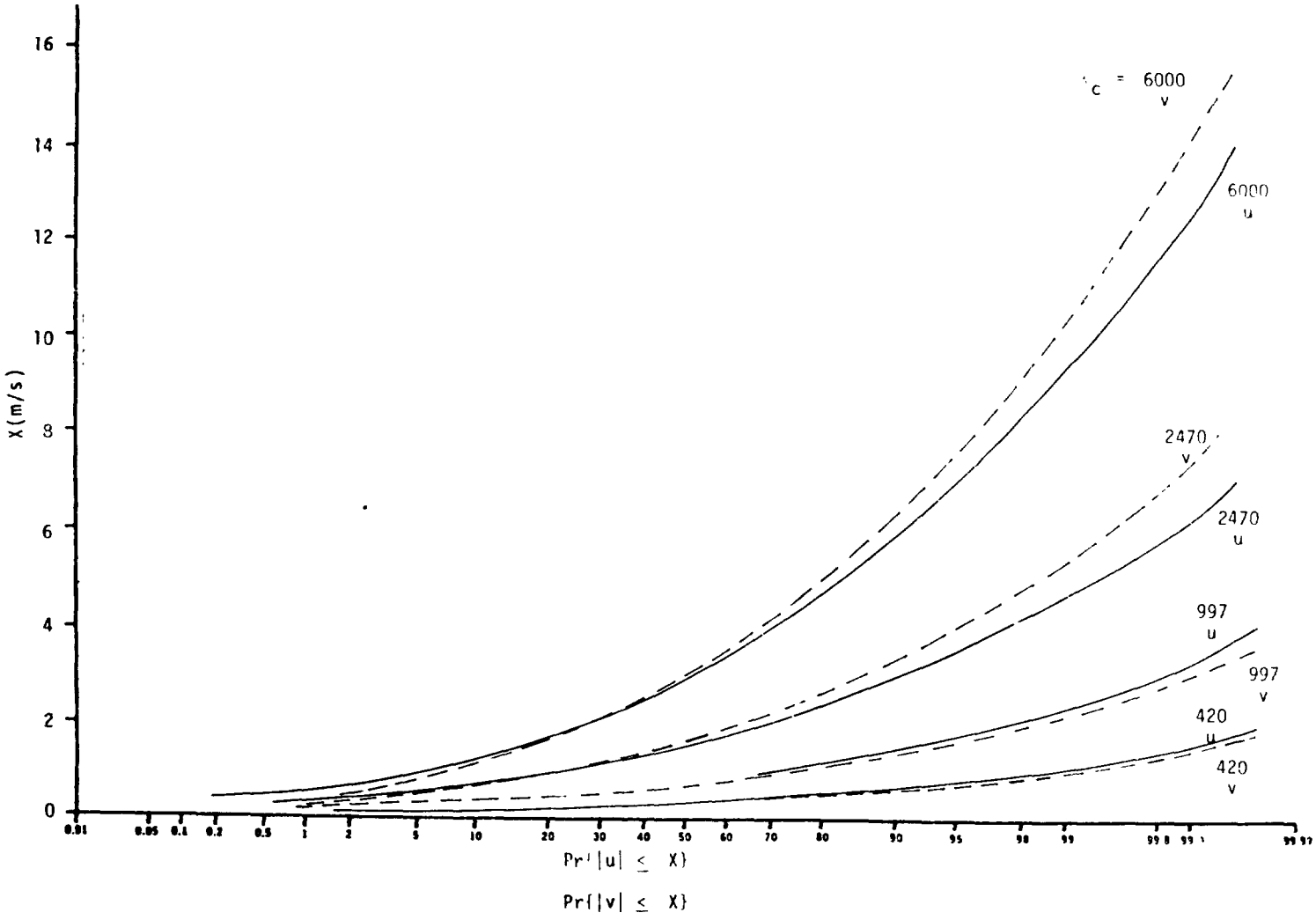

Figure 26. Theoretical Distributions of u and v Component Gust at 8 km for Various Filter Cut-off Wavelengths, λ_c

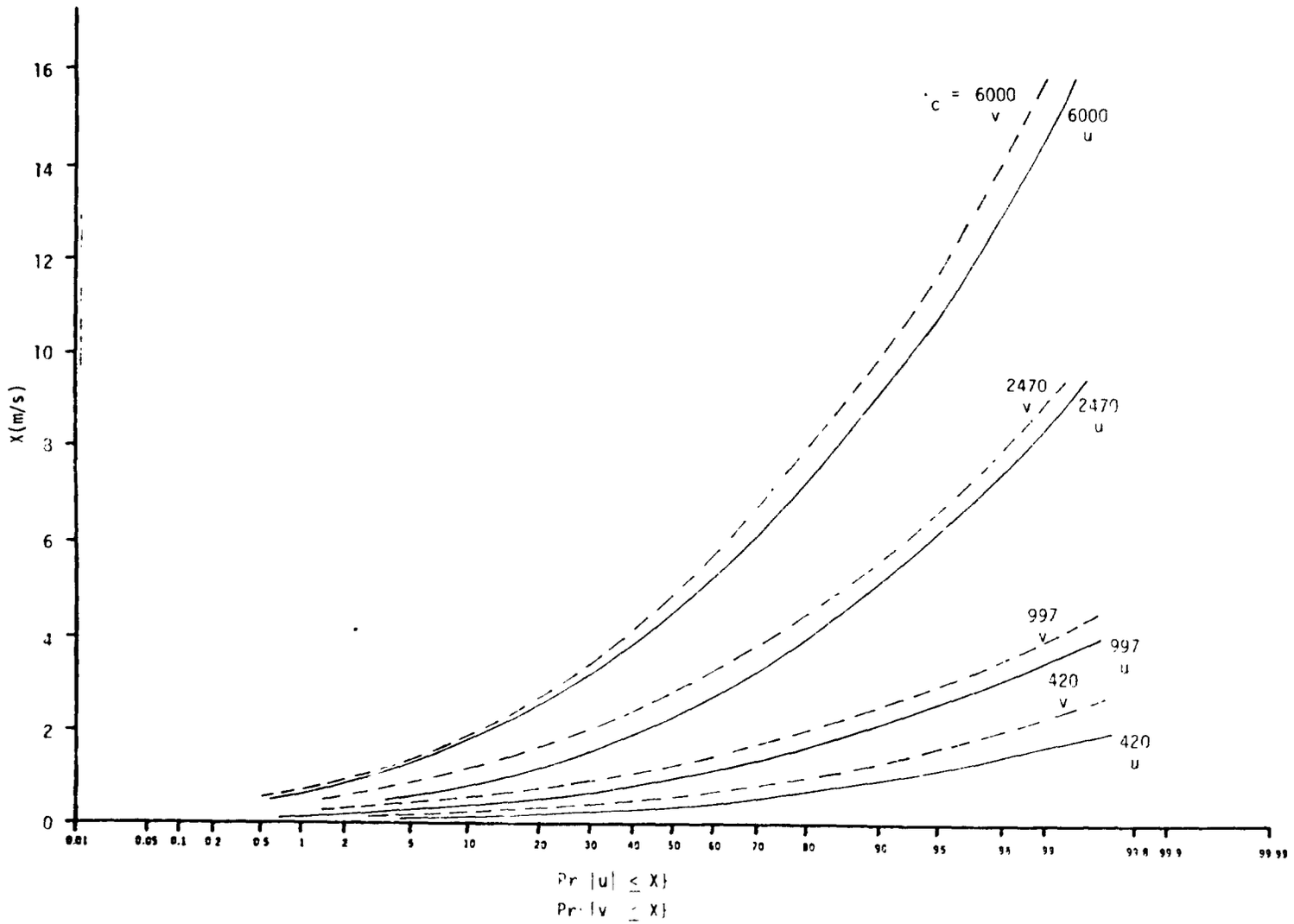

Figure 27. Theoretical Distributions of u and v Component Gust at 12 km for Various Filter Cut-off Wavelengths, λ_c

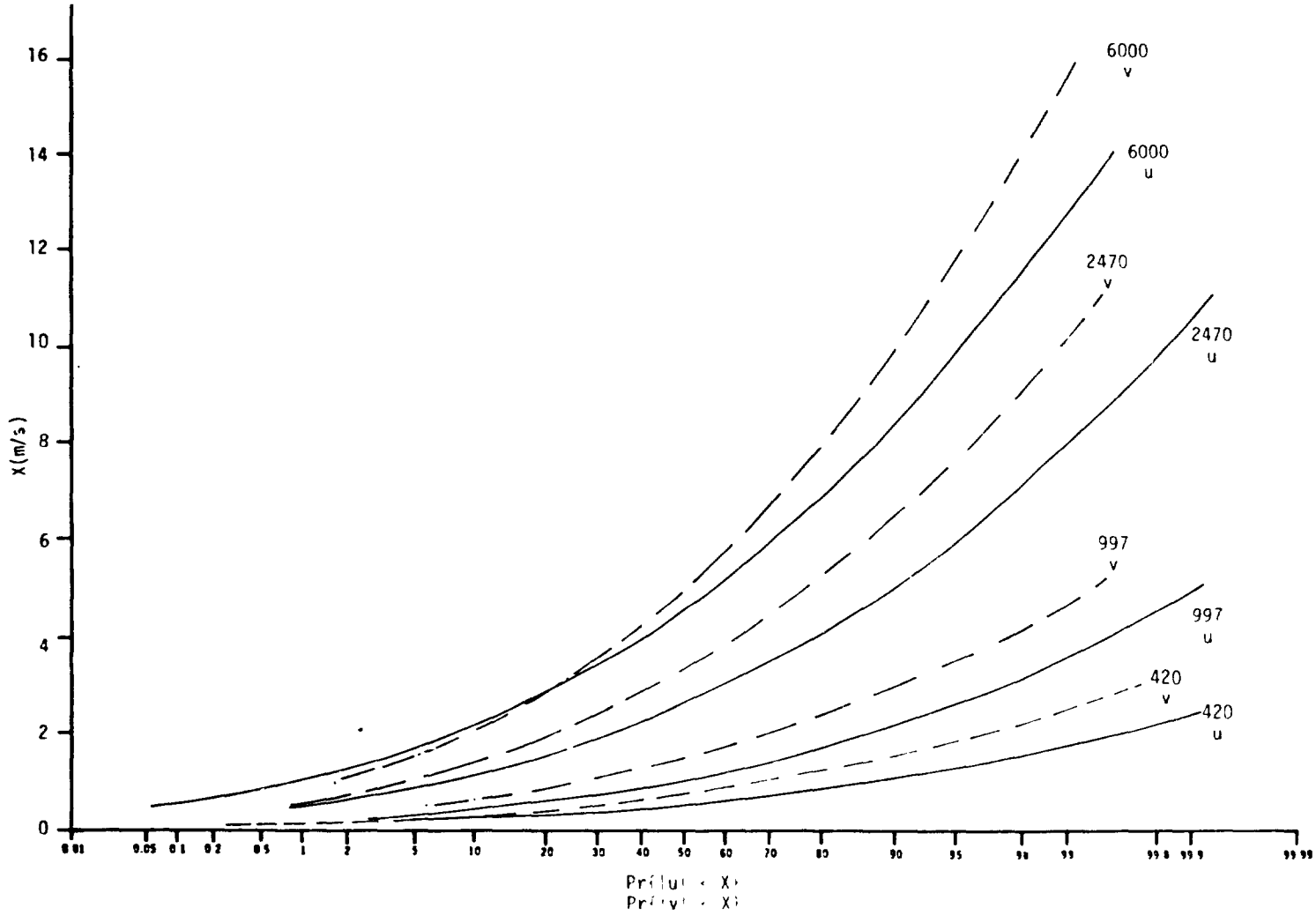

Figure 28. Theoretical Distributions of u and v Component Gust at 14 km for Various Filter Cut-off Wavelengths, λ_c

where T and w are the inverse of $|X'|_p$ and λ_c, respectively. A list of parameters a and b, calculated in this manner from theoretical percentiles, is given in Table 3. Curves representing Equation 16 for the 50, 90, 95, and 99 percentile gust components during February at 12 km over Cape Kennedy are illustrated in Figures 29 through 31; for comparison, the theoretical percentiles are also shown as plotted symbols. It is indicated that Equation 16 provides a very good fit to the theoretical percentiles.

Another function which exhibits the desired asymptotic behavior is of the form

$$|X'|_p = d\, e^{-k/\lambda c} \qquad (18)$$

The constants d and k are also estimated by a least-squares technique. This function does not fit the observed data as well as Equation 16.

3. Conditional Gamma Distributions. Conditional probability distributions of component gust given gust length for u and v component gusts have been calculated by integration of the conditional gamma probability density function. Conditional probabilities of gust, given gust lengths of 0, 100, 200, 400, and 800 m for λ_c = 2470 m, are illustrated in Figures 32 and 33 for u and v component gusts, respectively. The distribution for zero gust length is a consequence of the theoretical model and cannot be supported by available data.

4. Distribution of Differences Between the Altitudes of Zonal and Meridional Gust Components. It follows from the definition of gust used in this study that zonal and meridional gusts do not necessarily occur at the same altitude. The altitude difference, ΔH, between the gust components is a measure of phase difference. As illustrated in Figure 34, the distribution of ΔH can be accurately represented by a normal distribution; it is indicated that ΔH increases as filter cut-off wavelength, λ_c, increases. Theoretical distributions of ΔH for February and July at a reference altitude of 12 km are illustrated in Figure 35; ΔH is generally larger during July especially for larger values of λ_c. The variation of ΔH with altitude is illustrated in Figure 36;

Table 3. Parameters a and b of Equation 17 for Calculation of Gust Component Percentiles (m/s) at 12 km During February, April, and July at Cape Kennedy, Florida

	50	90	95	99	Percentile
			February		
			u Component		
a(s/m)	.0777	.0461	.0398	.0310	
1/a (m/s)	12.87	21.68	25.12	32.20	
b(s)	909.57	409.57	339.04	244.64	
			v Component		
a	.1228	.0647	.0552	.0419	
1/a	8.14	15.46	18.12	23.87	
b	592.51	276.04	229.65	167.86	
			April		
			u Component		
a	.0725	.0517	.0467	.0380	
1/a	13.80	19.36	21.40	26.35	
b	1023.6	491.9	411.5	304.1	
			v Component		
a	.1171	.0681	.0588	.0456	
1/a	8.54	14.69	17.02	21.93	
b	817.06	359.43	296.06	212.57	
			July		
			u Component		
a	.1557	.1048	.0927	.0748	
1/a	6.42	9.54	10.79	13.38	
b	1522.9	705.51	586.51	427.89	
			v Component		
a	.1358	.0696	.0578	.0451	
1/a	7.36	14.36	17.29	22.16	
b	1510.9	761.95	648.64	484.47	

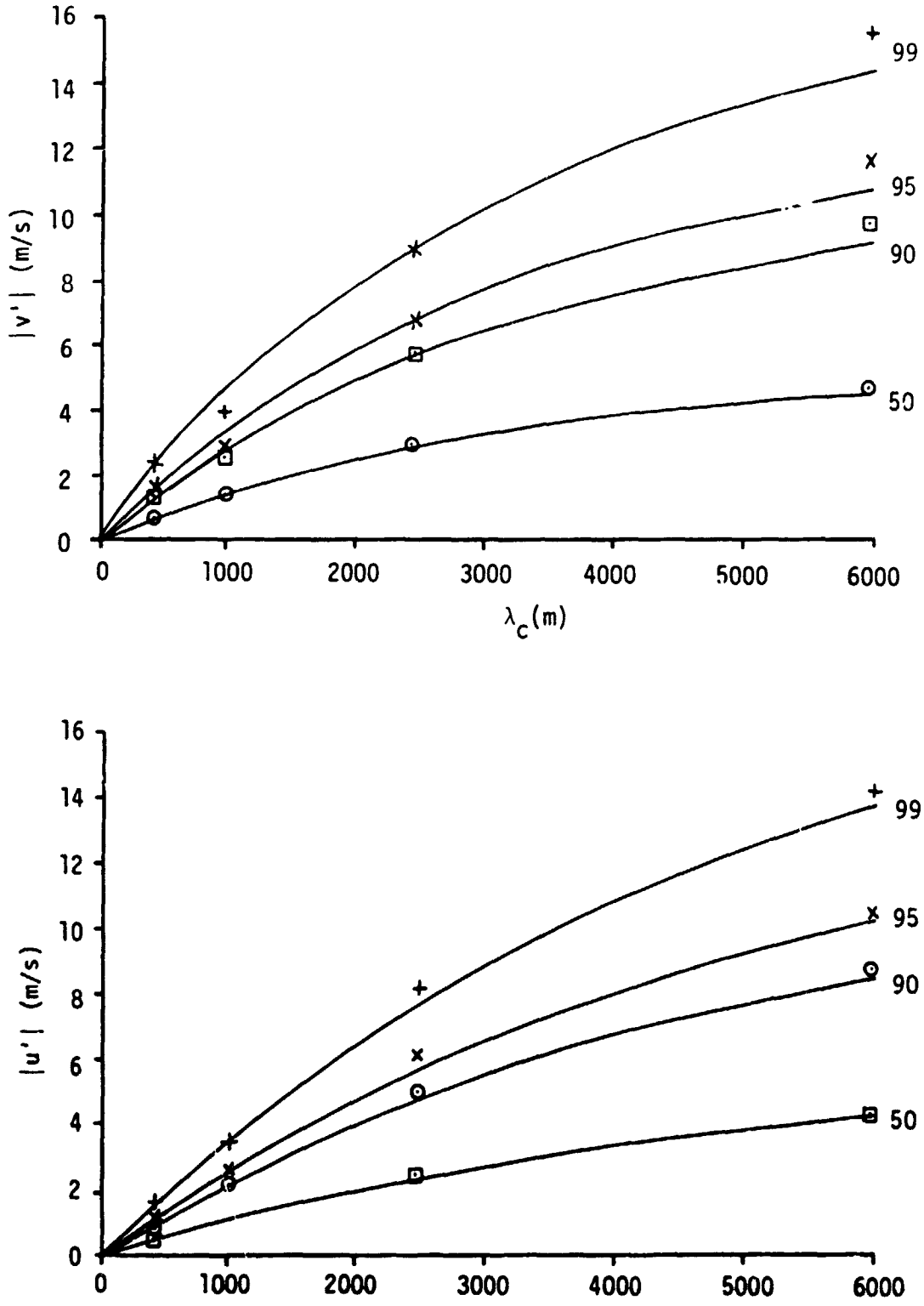

Figure 29. Theoretical 99, 95, 90, and 50 Percentile Component Gust (Curves Represent Equation 16) at 12 km During February at Cape Kennedy, Florida

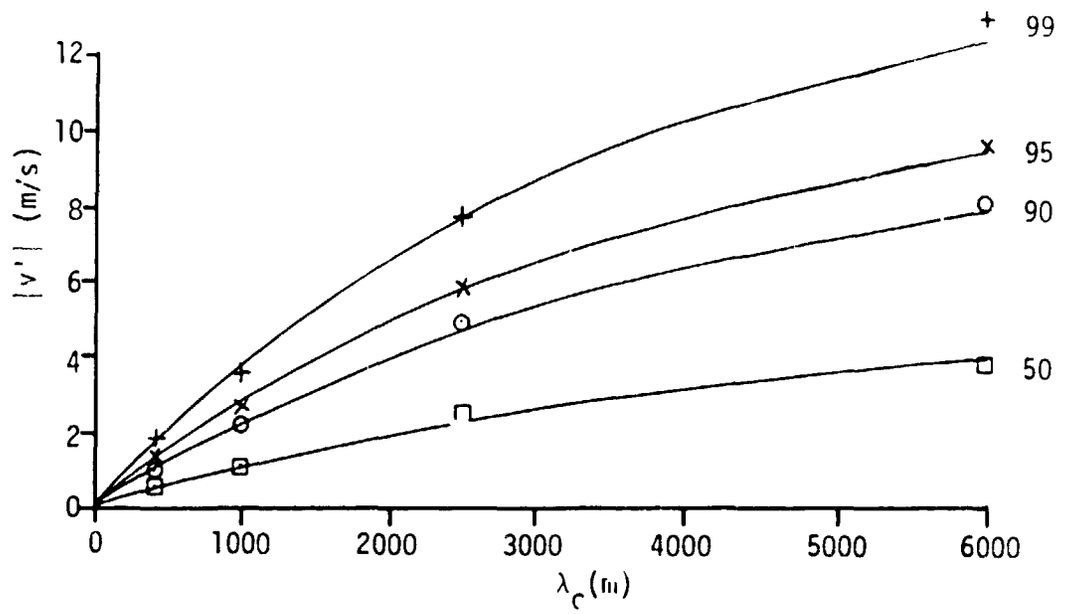

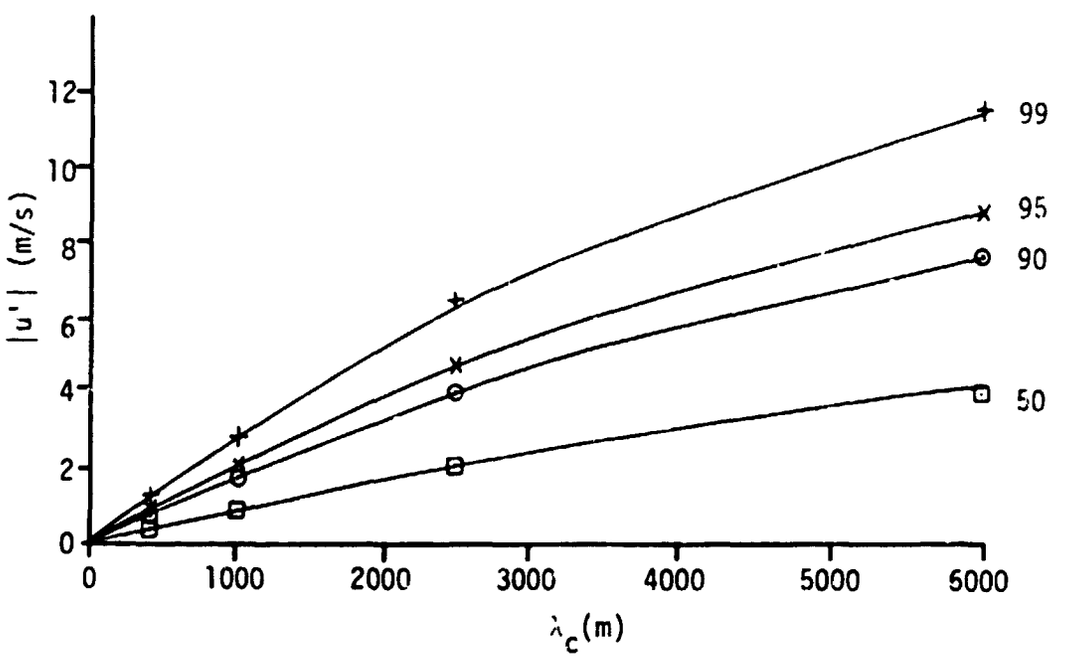

Figure 30. Theoretical 99, 95, 90, and 50 Percentile Component Gust (Curves Represent Equation 16) at 12 km During April at Cape Kennedy, Florida

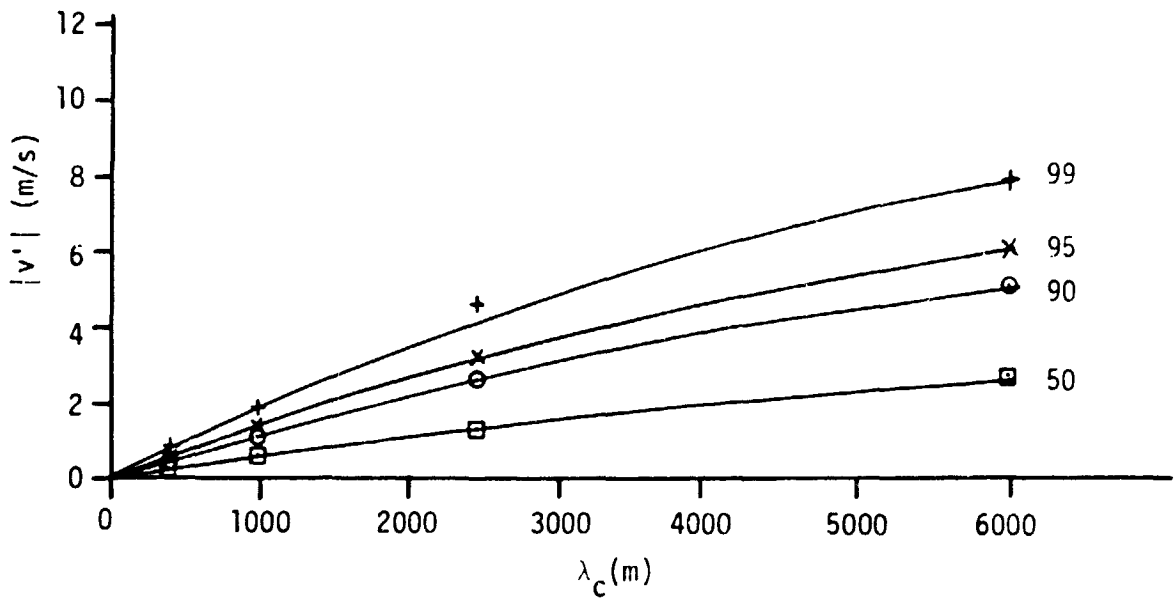

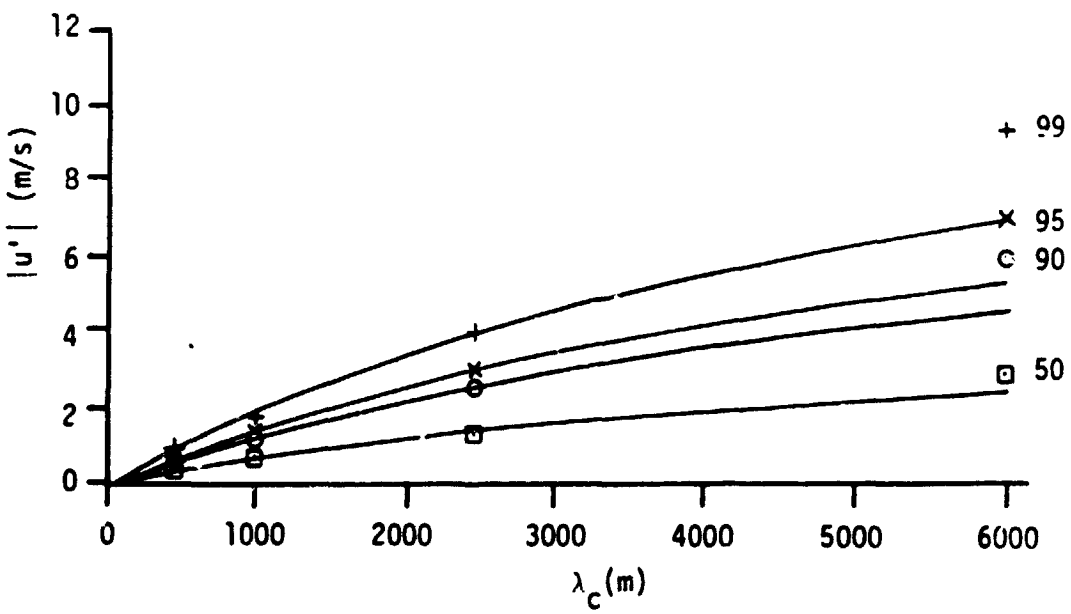

Figure 31. Theoretical 99, 95, 90, and 50 Percentile Component Gust (Curves Represent Equation 16) at 12 km During July at Cape Kennedy, Florida

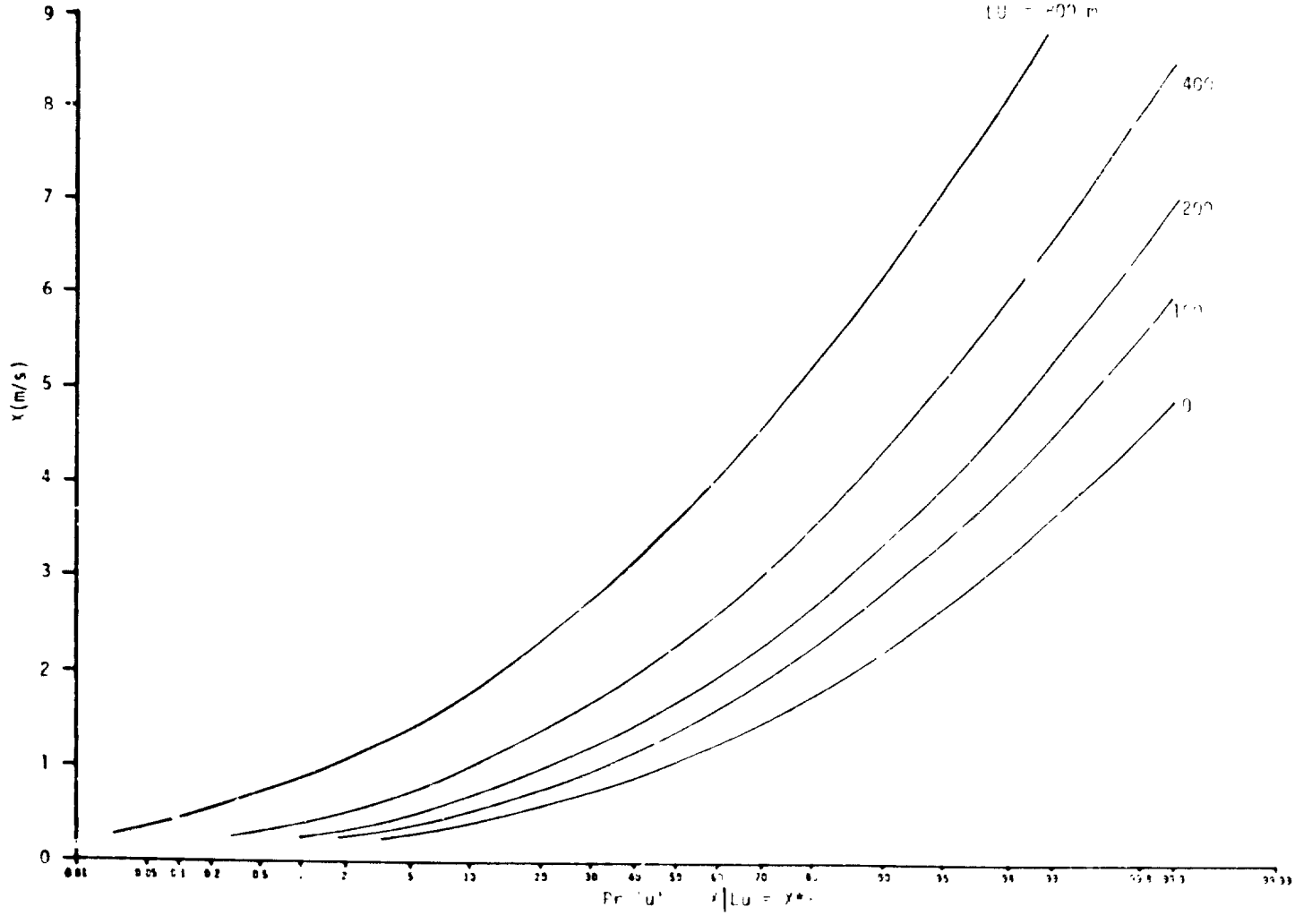

Figure 32. Theoretical Conditional Probability Distribution of u Component Gust Given Gust Length, LU

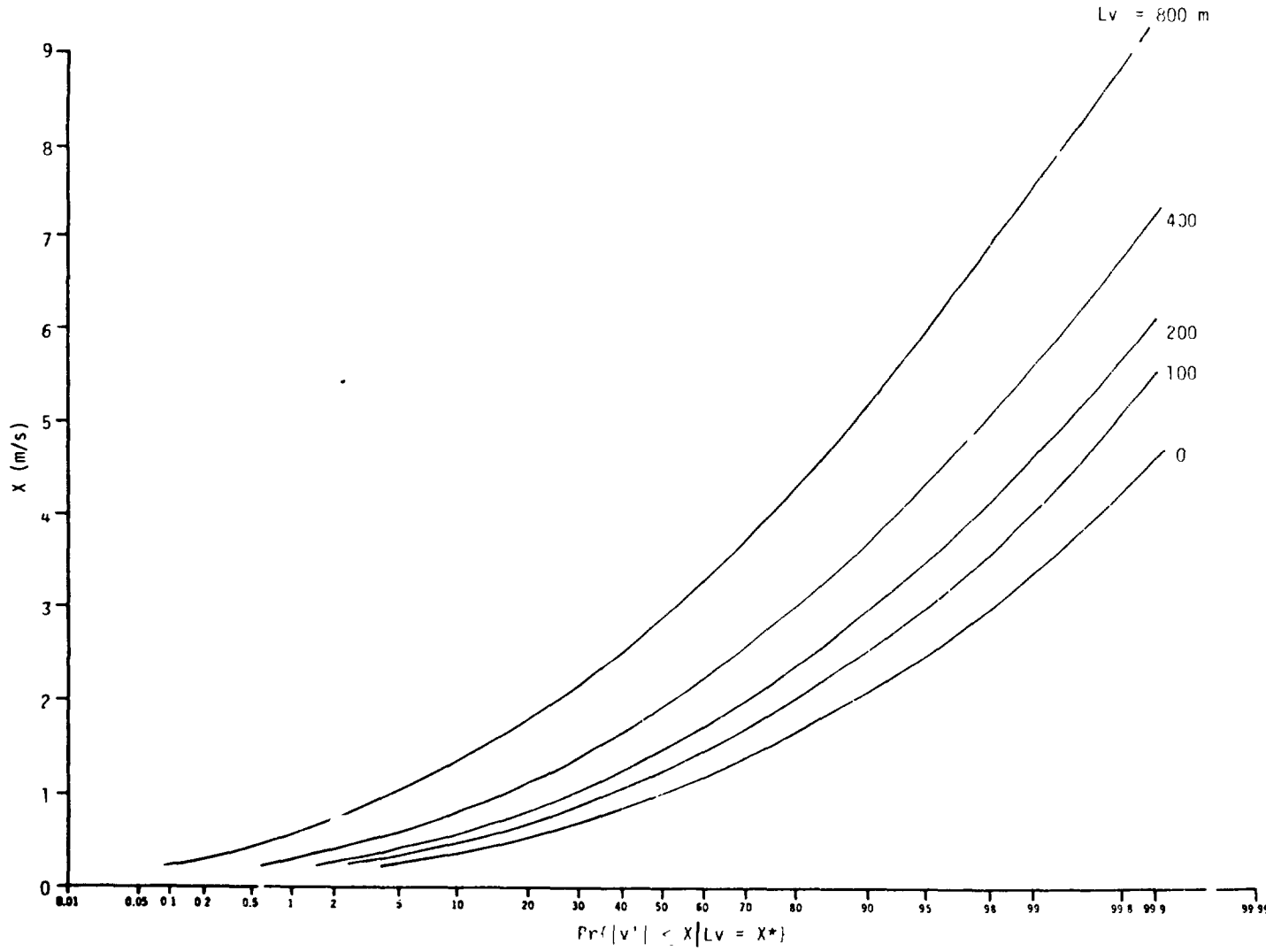

Figure 33. Theoretical Conditional Probability Distribution of v Component Gust Given Gust Length, Lv

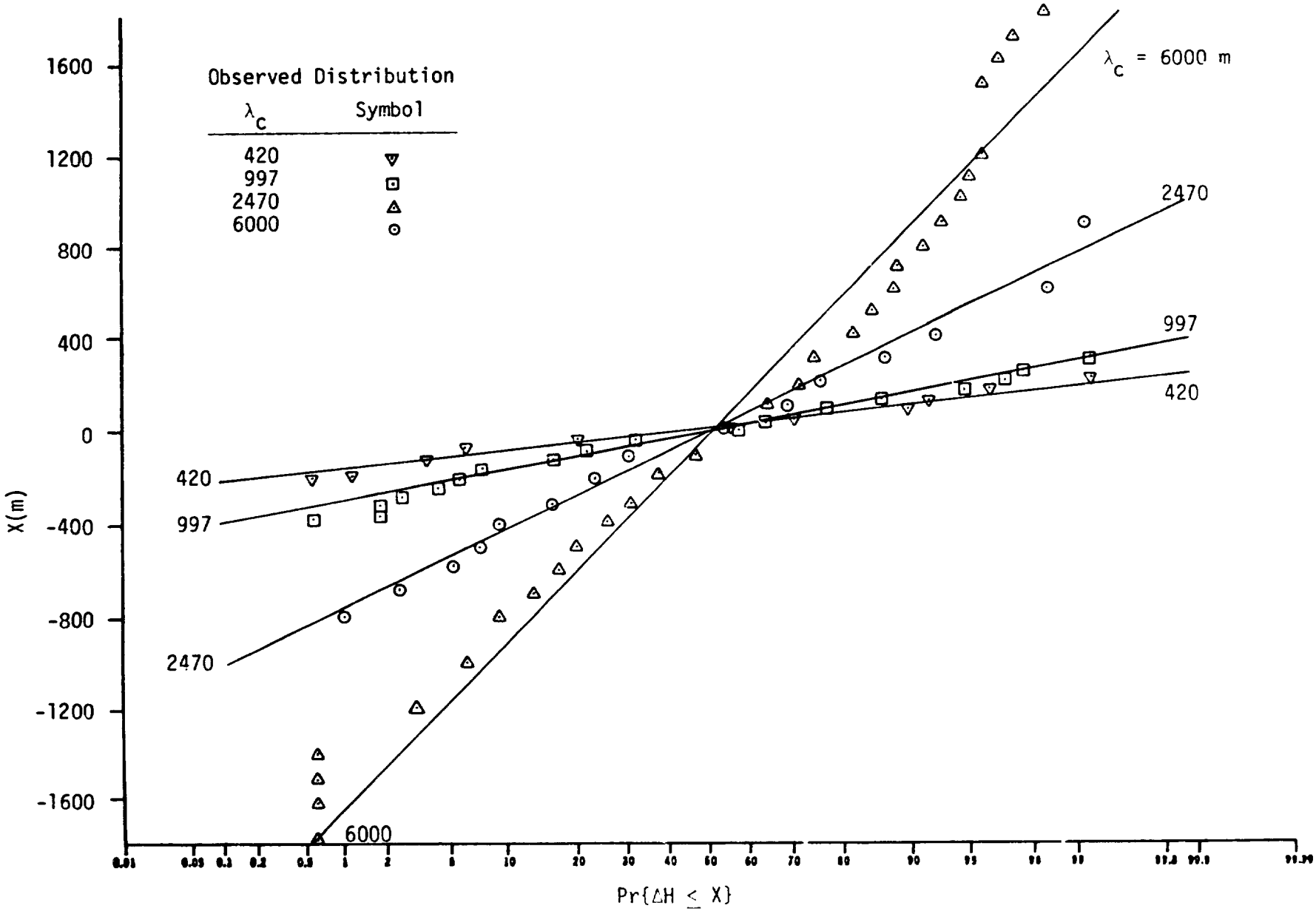

Figure 34. Observed and Theoretical (Normal) Probability Distribution of the Altitude Difference, ΔH, Between u and v Component Gust During February at Cape Kennedy (Reference Height = 12 km)

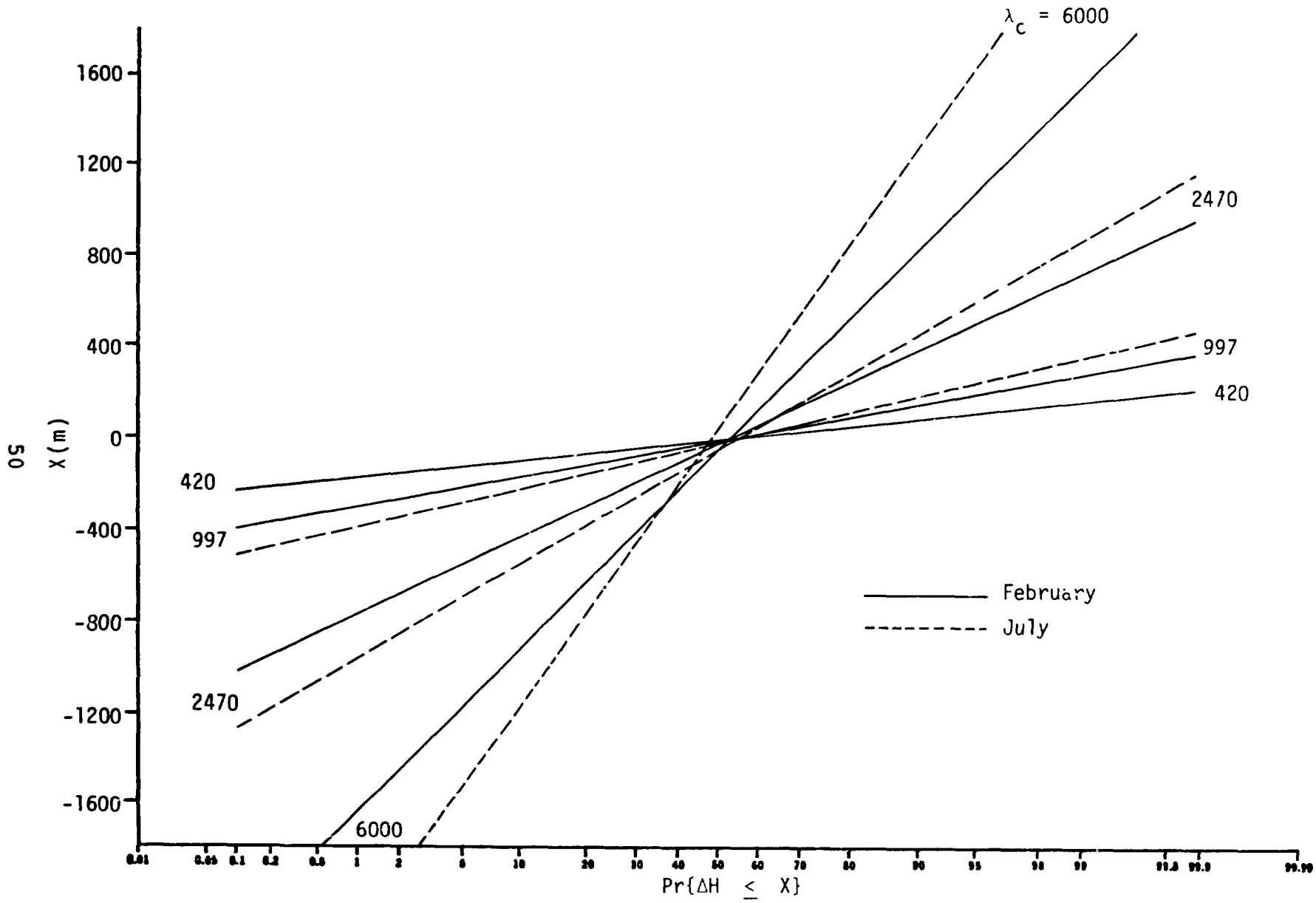

Figure 35. Theoretical (Normal) Probability Distribution of ΔH During February and July at a Reference Height of 12 km

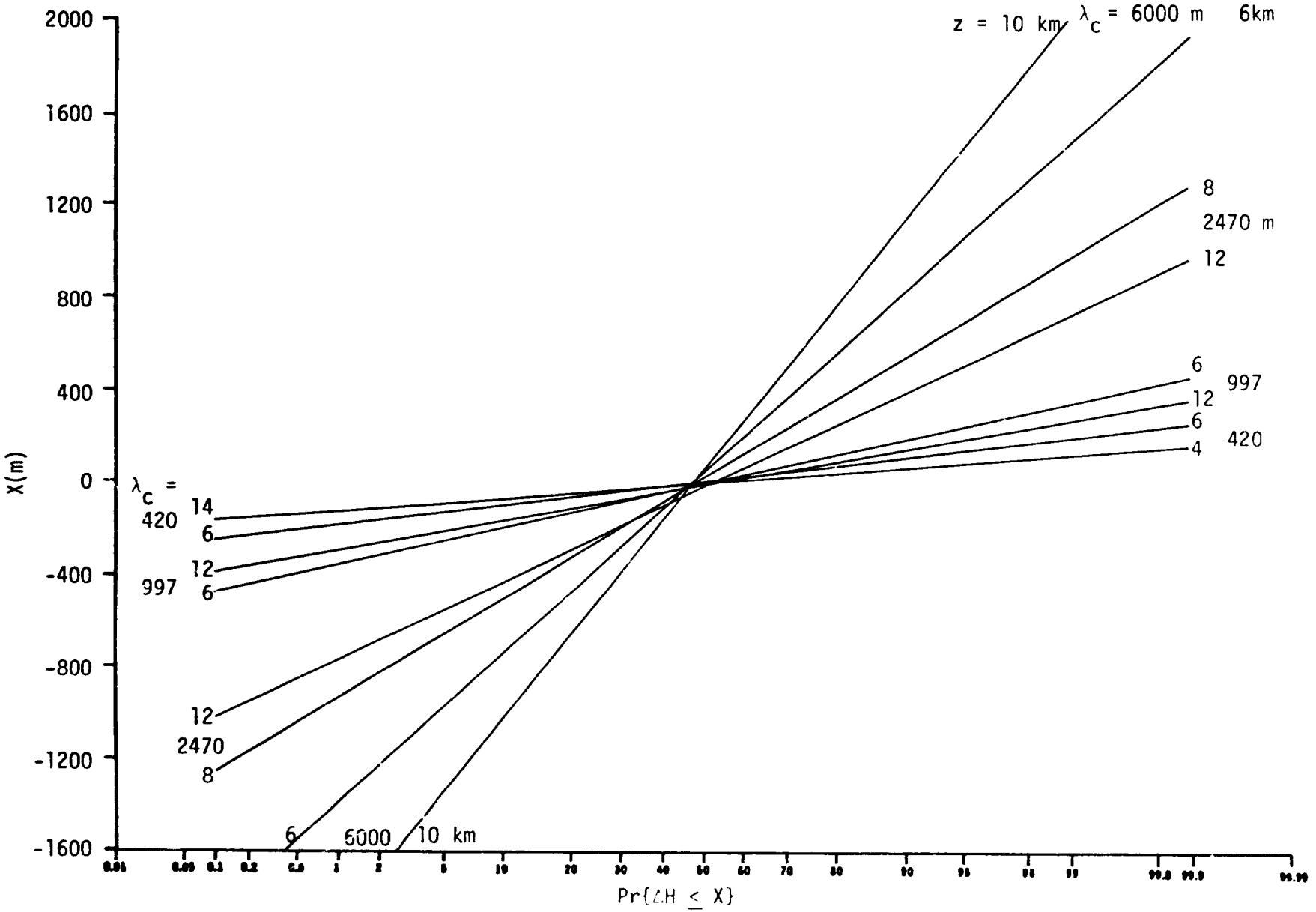

Figure 36. Theoretical (Normal) Probability Distribution of the Altitude Difference, ΔH, Between u and v Component Gust During February at Cape Kennedy as a Function of Reference Altitude

the theoretical distribution at the various altitudes were selected to illustrate the maximum variation of ΔH distributions within the 4 to 14 km altitude range. The variation of ΔH with altitude is not consistent with respect to the various filter cut-off wavelengths; i.e., to produce the maximum variation with respect to the six reference altitudes, different altitude combinations are required for each type of filtered data.

E. Distribution of Extreme Gust Modulus

Gust, as represented in this analysis, is a two-dimensional vector with components, u' and v', and modulus, R, given by

$$R = \sqrt{(u')^2 + (v')^2} \tag{19}$$

The largest value of R in a gust profile is the extreme gust modulus, R_{max}. A number of samples of R_{max}, each of size, n, equal to 150 have been generated from filtered wind profiles for the months of February, April, and July. The analysis described in this section is concerned with utilizing these samples to establish a theoretical probability distribution for R_{max}.

It is proposed that the distribution of R_{max} is the first asymptotic extreme value distribution described by Gumbel (10); this distribution, which is also known as the Fisher-Tippette Type I probability distribution is given by

$$\Phi(X) = e^{-e^{-y}} \tag{20}$$

where y is the reduced variate.

$$y = \alpha(X - \mu) \tag{21}$$

The parameters α and μ are estimated from the sample mean, $\bar{X}$, and the sample standard deviation, S_x.

$$\hat{\alpha} = \frac{\sigma_N}{S_x} , \qquad \hat{\mu} = \bar{X} - \frac{\bar{y}_N}{\hat{\alpha}} \tag{22}$$

where σ_N and $\bar{y}_N$ are population mean and standard deviation which are a function of sample size; for n = 150 Gumbel's tabulation (Ref. 10) has $\sigma_N = 1.22534$ and $y_N = .56461$.

The variable X in Equation (20), which herein represents R_{max}, can be calculated from the reduced variate according to the equation

$$X = \hat{\mu} + \frac{y}{\hat{\alpha}} \tag{23}$$

Table (4) contains the values of $\hat{\mu}$ and $1/\hat{\alpha}$ that have been calculated from samples of R_{max} during February, April, and July as a function of filter wavelength cut-off, λ_c.

The function represented by Equation (23) appears as a straight line when plotted on extreme value probability graph paper. The theoretical distributions of R_{max} during February for four filter cut-off wavelengths are illustrated in Figure 37; the observed distributions, represented by the plotted symbols in Figure 37, do not deviate significantly from the theoretical lines.

Table 4. Sample Means and Standard Deviations of R_{max} and Estimates of Parameters $1/\alpha$ and μ of the First Asymptotic Extreme Value Distribution (Gumbel, Ref. 10) for n = 150, σ_N = 1.22534 and $\bar{y}_N$ = .56461

λ_c(m)	420			997			2470			6000		
Month	Feb	Apr	Jul	Feb	Apr	Jul	Feb	Apr	Jul	Feb	Apr	Jul
$\bar{X}$(m/s)	2.465	2.303	1.808	3.973	4.116	3.339	7.122	7.111	5.491	10.070	9.509	7.447
S_x(m/s)	.628	.425	.348	.724	.712	.743	1.498	1.346	1.171	2.608	2.160	1.926
$\hat{1/\alpha}$(m/s)	.513	.347	.284	.591	.581	.606	1.225	1.098	.955	2.128	1.763	1.572
$\hat{\mu}$(m/s)	2.176	2.107	1.648	3.639	3.788	2.997	6.432	6.491	4.951	8.868	8.514	6.560

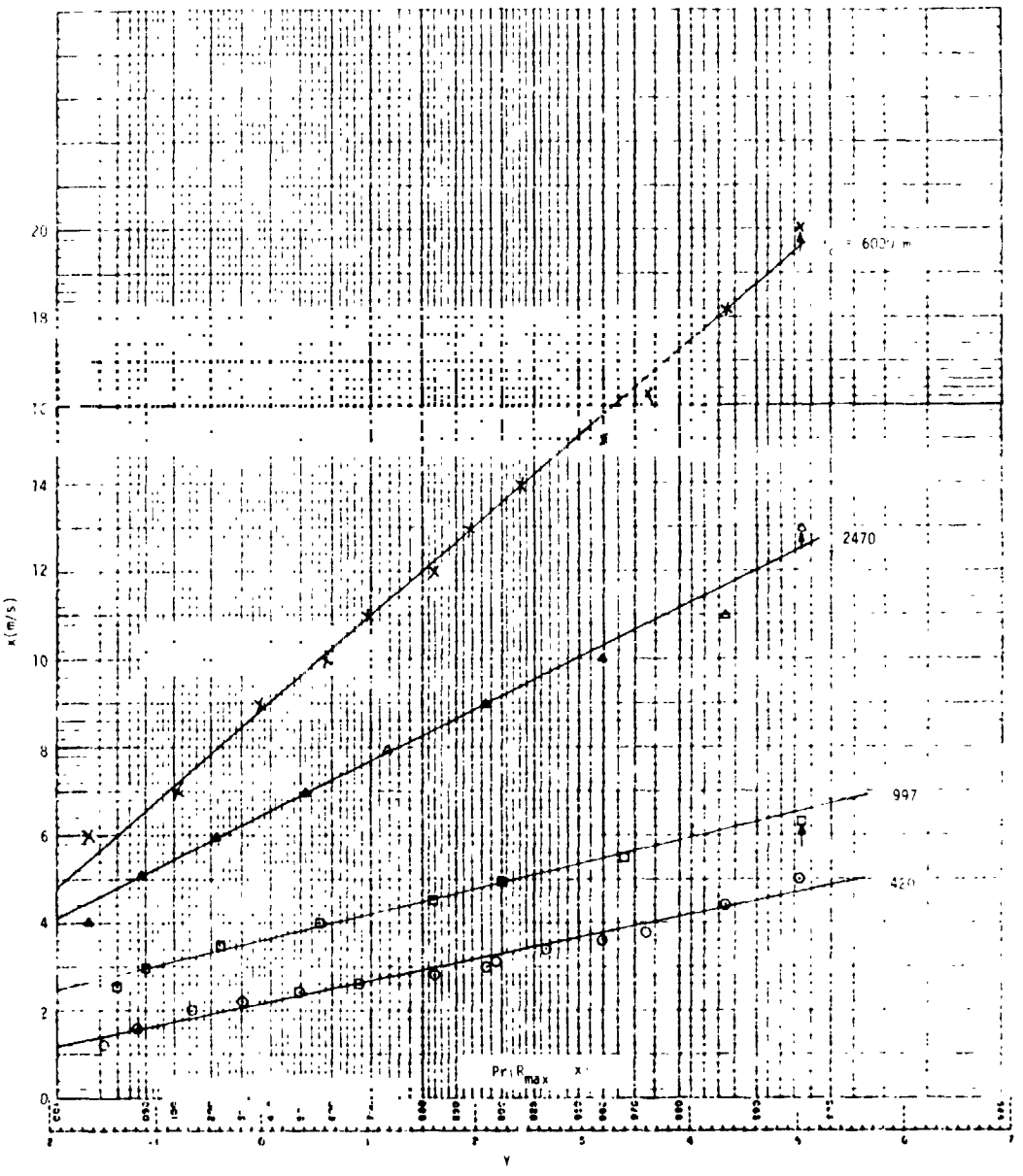

Figure 37. Observed (Plotted Symbols) and Theoretical Distribution (Extreme Value) of R_{max} During February at Cape Kennedy for Various Filter Cut-off Wavelengths, λ_c

SECTION IV. CONCLUSIONS

The results of this study provide the basis for a vector wind model for Cape Kennedy, Florida. A methodology has been developed for the derivation and analysis of small-scale perturbations in Jimsphere wind profiles. Gusts in various wavelength bands have been derived from these perturbations; the probability distribution of gust components and associated gust length has been shown to be accurately represented by a gamma distribution. Theoretical and observed distributions of component gust vary significantly with season, altitude, and wavelength range.

SECTION V. REFERENCES

1. Jones, J. C.: A Unified Discrete Gust and Power Spectrum Treatment of Atmospheric Turbulence. International Conference on Atmospheric Turbulence, London, England, May 1971. (AIAA Reprint No. A71-29790.)

2. Brown, S. C.: 150 Per Month Jimsphere Wind Speed Profiles for Aerospace Vehicle Design Capability Studies, KSC, Florida. NASA Document NASA/MSFC-ES81, February, 1978.

3. Adelfang, S. I., and Court, A.: Jimsphere Wind and Turbulence Exceedance Statistics. NASA CR-2118, NASA, Washington, D.C., August 1972.

4. Luers, J., and Engler, N.: On Optimum Methods for Obtaining Wind Data from Balloon Sensors. Journal of Applied Meteorology, Vol. 6, No. 5, October 1967, pp. 816-823.

5. DeMandel, R. E., and Krivo, S. J.: Study to Improve the Accuracy and Resolution of FPS-16 Radar/Jimsphere Wind Measurements. Lockheed Missiles and Space Company Final Report under NASA Contract NAS8-26128, June 1971.

6. DeMandel, R. E., and Krivo, S. J.: Selecting Digital Filters for Application to Detailed Wind Profiles. NASA CR-61325, 1971.

7. Thom, H. C. S.: Some Methods of Climatological Analysis. WMO Technical Note 81, WMO-MO.199.TP.103, 1966.

8. Bury, K. V.: Statistical Models in Applied Science, Wiley, New York, 1975.

9. Mann, N. R., Schafer, R. E., and Singpurwalla, N. D.: Methods for Statistical Analysis of Reliability and Life Data, Wiley, New York, 1974.

10. Gumbel, E. J.: Statistics of Extremes, Colombia University Press, New York, 1958.